University of Iceland
Faculty of Natural Science
Department of Physics

RH-08-2004

Manipulating the Persistent Current in Quantum Rings

by

Sigríður Sif Gylfadóttir

A thesis submitted in partial satisfaction of the requirements for the degree of Master of Science in Physics at the University of Iceland

Committee in charge:
Prof. Viðar Guðmundsson, Chair
Dr. Andrei Manolescu

Reykjavík
June 2004

Manipulating the Persistent Current in Quantum Rings

Printed in Iceland by Prentmet

Abstract

The properties of a one-dimensional quantum ring are investigated, in particular the persistent current which appears when the ring is placed in an external magnetic field. The Coulomb interaction between electrons is included within the Hartree-Fock approximation. By applying a strong and short-lived pulse of radiation a dynamic current, different from that of the ground state, can be induced. The current is changed through a modification of the many-electron state of the system. The effects of asymmetry are discussed and the possibility to induce a current on the ring in a zero magnetic field.

Útdráttur

Eiginleikar einvíðs skammtahrings eru skoðaðir og sérstök áhersla lögð á sístæða strauminn sem kemur fram þegar hringurinn er í ytra segulsviði. Áhrif víxlverkunar á kerfið eru könnuð innan Hartree-Fock nálgunarinnar. Þegar örskammur geislunarpúls verkar á kerfið breytist fjöleindaástand þess, og með því móti má breyta straumnum á hringnum. Áhrifum ósamhverfu, annars vegar með því að örva hringinn með ósamhverfri truflun og hins vegar með því að móta hringinn með ósamhverfu bakgrunnsmætti, er lýst.

Contents

Acknowledgments

There are inevitably many people which influence work of this kind, whether professionally or personally. The list could go on for pages and include remarks such as "Thanks to all the great physicists who paved the path for me to follow". But one does not want to scare away potential readers before the arabic page numbering starts.

First and foremost I would like to express my deepest gratitude to my supervisor Prof. Viðar Guðmundsson whose encouragement, patience and excellent guidance made this work possible. Dr. Andrei Manolescu's and Dr. Snorri Ingvarsson's sharp observations and clever suggestions were also most appreciated. I have been so fortunate to spend a year in a nice little cubicle along with Jens Hjörleifur Bárðarson, my co-student. Sharing thoughts and questions about physics with him has been very rewarding, but I must also stress that discussing everyday trivia, exchanging jokes and even occasionally political opinions, have made this year at the "office" incredibly fun.

During a stay in Helsinki, Academy Prof. Risto Nieminen and Dr. Ari Harju kindly gave me an opportunity to work at the Laboratory of Physics at the Helsinki University of Technology, where parts of this work were done.

My family has had a big part in getting me here, both physically and mentally. For this I am very grateful. My friends have also followed me all the way here and will hopefully continue to do so for many years. Without them, no matter how exciting physics can be, life would indeed be very dull.

Last but not least, thank you Frank for making me happy.

Chapter 1

Introduction

For the past two decades low-dimensional electron systems, such as quantum dots and rings, have been the subject of considerable interest and studied extensively. These small structures are, amongst other methods, formed in a two-dimensional electron gas by applying appropriate confinement, thus restricting the motion of electrons in all three dimensions to a small area on the boundary between two semiconducting materials [1]. Due to their small size (on the nanometer scale), these systems are governed by quantum effects and thus, their energy spectrum is discrete. They are in many ways similar to atoms, however, their properties can be controlled by adjusting their geometry, the confinement and applied magnetic field. Nanostructures are a source of discoveries of intruiging quantum phenomena which do not appear in atoms. They are important both in connection with potential device applications and can function as convenient samples to probe the properties of many-electron systems in reduced dimensions.

The quantum ring is a system of electrons confined to a circular region. When it is placed in an external magnetic field perpendicular to the plane in which it lies, a constant current flows along the ring. The possibility of circulating currents in sufficiently small rings and cylinders was first proposed in the late 1960's following investigations into magnetic flux quantization in superconducters [2–5]. Two decades later the persistent current in small rings made from normal metals was established [6–8] and the effect of scattering as well as finite temperature upon it. The persistent current was shown to be periodic in the magnetic flux threading the ring, with a period of the flux quantum $\Phi_0 = h/e$ [6, 7, 9] (full period oscillations), even in the presence of elastic scattering. In fact, many of the physical properties of the one-dimensional quantum ring are periodic in the magnetic flux, a manifestation of the Aharonov-Bohm effect [10] as well as the one-dimensionality. The properties of rings of finite width are quasi-

periodic in the magnetic flux.

A few years earlier, dirty metal cylinders and arrays of rings were found to exhibit oscillations in the conductivity with a period of half a flux quantum $\Phi_0/2$ (half period oscillations), both in theory [11] and experiment [12–14]. For some time, the existence of Φ_0 oscillations was debated, as it had not been observed in experiments. In 1985, Webb et al. [15] measured full period oscillations in the magnetoresistance of gold rings as well as weaker half period oscillations. The amplitude of the oscillations was studied as a function of temperature by Washburn et al. [16]. Shortly afterwards $\Phi_0/2$ resistance oscillations were reported for single aluminium and silver rings with Φ_0 oscillations in the former at higher magnetic fields [17]. In an experiment with arrays of gold rings, Umbach et al. [18] showed that the Φ_0 periodicity gradually disappeared with an increased number of rings, but the half period oscillations persisted. Much discussion on the origin of these two oscillation modes took place, with emphasis on the effect of ensemble averaging, either over a distribution of random disorder [19–24], energy, or the different number of particles on rings in arrays. Stone et al. [25] found that the full and half period oscillations in single rings have different sensitivities to the temperature and magnetic field. For low temperatures the full period oscillations are dominant, but at higher temperatures the half period oscillations dominate at low fields, giving way to weaker full period oscillations at high magnetic fields. The effects of temperature and disorder were found by Cheung et al. [26] to exponentially reduce the persistent current and due to averaging over an ensemble of rings containing different numbers of particles, the periodicity changes to $\Phi_0/2$. Montambaux et al. [27] showed that the ensemble average of the current over disorder or the number of particles leads to half period oscillations. Diffusion and increased number of channels were found to reduce the average current. Measurements on an array of 10^7 copper rings showed that the oscillations had a $\Phi_0/2$ periodicity [28]. In 1991 measurements on a single gold ring found a Φ_0 periodicity of the persistent current, but its magnitude was 1-2 orders of magnitude larger than that predicted by theory [29]. This discrepancy between measurement and theory in mesoscopic rings has not yet been resolved. The inclusion of the electron spin was shown to reduce the period and amplitude of the persistent current. The effect depends strongly on the number of electrons N_e on the ring and leads to strong fluctuations between samples [30]. These results are a strong indication that the two oscillation modes are caused by different mechanisms. The half period oscillations originate in mesoscopic effects such as disorder, which eliminate the full period oscillations caused by the geometry of the quantum ring.

Experimental results for mesoscopic quantum rings made in GaAs/AlGaAs semiconductor heterostructures were reported by Timp et al. [31] in 1987. The magnetoresistance oscillated with a period Φ_0. Since then, several experiments on semiconductor quantum rings were conducted [32–44] and in 2000 the nanoscale was reached by Lorke et al. [45].

Since the early 1990's, research on quantum rings has expanded rapidly. The work has been varied, as an example one can specify studies of optical properties [46–48], the effect of impurities [49–53], current magnification in open rings [54, 55], and magnetization and its relation to the persistent current [56, 57]. The effect of the electron-electron interactions has been of particular interest and considered a good candidate to explain the large discrepancy between theory and experiments on mesoscopic rings. A controversy exists, the Coulomb interaction is seen to both enhance and suppress the persistent current and to have no effect at all [51–53, 58–62]. The effect of the Coulomb interaction on the periodicity of the persistent current and energy spectrum of the quantum ring has also been studied extensively [63–66], and shown to lead to oscillations of period Φ_0/N_e where N_e is the number of electrons.

Over the past few years an interest in time-dependent or radiation induced phenomena in various mesoscopic electron systems has emerged [67–82]. Very recently, Luo et al. [80] reported on the generation of THz pulses with field amplitudes up to several MV/cm, allowing for nonlinear THz spectroscopy which was used to study Rabi oscillations in GaAs/AlGaAs quantum wells. It is likely that more experimental studies of nonlinear excitations of nanostructures will follow, and in the future open up a new and exciting field.

The main topic of this thesis is the effects of a nonlinear radiation pulse in the THz frequency range upon the persistent current of a semiconductor quantum ring on the nanometer scale. In Chapter 2 the ground state of the ring will be described, first when the Coulomb interaction between electrons and their spin is neglected, and following that with interaction and spin included within the Hartree-Fock approximation. The ground state persistent current is then discussed and compared for the two cases. Chapter 3 deals with the effects of a time-dependent perturbation on the persistent current and electron density, and Chapter 4 investigates the possibilities of generating a steady current at a zero magnetic field.

Chapter 2

Ground State Properties

The quantum ring is a system that displays many intriguing properties of which the persistent current will be central to this thesis. Despite its apparent simplicity, the many-electron Schrödinger equation of the one-dimensional ring is complicated and its analytic solutions unknown. Furthermore, an accurate description of the system is complicated due to the strength and behaviour of the Coulomb interaction in one dimension.

In this chapter the ground state properties of the one-dimensional quantum ring will be investigated, starting from a simple single-electron model and working our way towards a more accurate but complex model of the system. First the analytic solutions of the Schrödinger equation of the ring, neglecting interactions between electrons as well as their spin, will be derived. The density matrix is then introduced and will be used extensively in the formulation of a more accurate description of the system, the many-electron Hamiltonian. The analytical solution of the many-electron Schrödinger equation does not exist. Due to its complexity, solving it numerically is impractical and even impossible except for very few electrons. Therefore, a method of simplification or approximation must be used, one of which is the Hartree-Fock approximation. The method is described as well as its practical implementation. Following that the ground state energy spectrum of the one-dimensional interacting ring, as obtained within the Hartree-Fock approximation, is depicted and its properties discussed. The final section of the chapter is devoted to a special ground state property of the quantum ring, the persistent current.

2.1 THE NONINTERACTING QUANTUM RING

The noninteracting one-dimensional (spinless) electron gas on a ring is a system whose equation of motion, the Scrödinger equation, has a known analytical solution. In this section we derive the ground state properties of the ring when placed in a constant magnetic field perpendicular to the plane in which the ring lies.

The Hamiltonian of a system of noninteracting electrons in an external magnetic field $\mathbf{B}$ is a sum of single-particle Hamiltonian operators, the effective kinetic energy of the electrons,

$$H = \sum_i h_i = \sum_i \frac{1}{2m^*} \left(\mathbf{p}_i + e\mathbf{A}\right)^2, \tag{2.1}$$

where m^* denotes the effective electron mass, $\mathbf{p}_i$ the momentum of electron i and $\mathbf{A}$ a vector potential describing $\mathbf{B}$

$$\mathbf{B} = \nabla \times \mathbf{A}. \tag{2.2}$$

The state vector of the system is composed of an antisymmetrized product of single-electron states that are solutions to the single-electron Schrödinger equation

$$h_0 \left|\phi_i\right\rangle = \epsilon_i \left|\phi_i\right\rangle, \tag{2.3}$$

where ϵ_i is the i-th energy eigenvalue of the Hamiltonian

$$h_0 = \frac{1}{2m^*} \left(\mathbf{p} + e\mathbf{A}\right)^2. \tag{2.4}$$

The electrons are confined to a ring of radius r_0. Assuming that the magnetic field is constant and perpendicular to the plane of the ring, the vector potential can be expressed in the symmetric gauge

$$\mathbf{A} = -\frac{1}{2}\mathbf{r} \times \mathbf{B} = \frac{r_0 B}{2}\, \hat{e}_\theta, \tag{2.5}$$

where $\hat{e}_\theta$ is a unit vector in the in-plane angular direction and B is the magnitude of the magnetic field, $B = |\mathbf{B}|$. In polar coordinates the Hamiltonian becomes

$$h_0 = -\frac{\hbar^2}{2m^* r_0^2} \left[\frac{\partial^2}{\partial\theta^2} + i\frac{eBr_0^2}{\hbar}\frac{\partial}{\partial\theta} - \left(\frac{eBr_0^2}{2\hbar}\right)^2\right]. \tag{2.6}$$

Using the magnetic flux

$$\Phi = \mathbf{B} \cdot \mathbf{S} = B\pi r_0^2 \tag{2.7}$$

as well as the flux quantum $\Phi_0 = h/e$, the Hamiltonian can be simplified to the form

$$h_0 = -\frac{\hbar^2}{2m^* r_0^2} \left[\frac{\partial^2}{\partial\theta^2} + 2i\,\frac{\Phi}{\Phi_0}\frac{\partial}{\partial\theta} - \left(\frac{\Phi}{\Phi_0}\right)^2\right]. \tag{2.8}$$

The time-independent Schrödinger equation of the system

$$\hat{h}_0 \, |\phi\rangle = \epsilon \, |\phi\rangle \tag{2.9}$$

has a known analytical solution and on imposing the boundary condition $\phi(\theta + 2\pi) = \phi(\theta)$ one finds that the eigenvalues of the Hamiltonian are restricted to a discrete set of allowed values. It also specifies the corresponding wave functions up to a multiplicative constant which is fixed by the normalization condition. The wave functions and single-particle spectrum of the one-dimensional ring are thus found to be

$$\begin{aligned} \langle \mathbf{r} \, |m\rangle = \phi_m(\theta) &= \frac{e^{-im\theta}}{\sqrt{2\pi r_0}}, \\ \epsilon_m &= \frac{\hbar^2}{2m^* r_0^2} \left(m - m_\Phi\right)^2, \end{aligned} \qquad m = 0, \pm 1, \pm 2, \ldots \tag{2.10}$$

where $m_\Phi = \Phi/\Phi_0$. The wave functions are eigenfunctions of the z component of the angular momentum $\hat{L}_z$ whose eigenvalues are determined by the quantum number m

$$\hat{L}_z \, |m\rangle = -m\hbar \, |m\rangle \, . \tag{2.11}$$

Therefore, m also indicates the z component of the angular momentum of the state. The set of wave functions $\{|m\rangle\}$ forms a complete orthonormal basis

$$\langle \, l \, |m\rangle = \delta_{lm}, \qquad \sum_m |m\rangle \, \langle m| = \mathbb{1}, \tag{2.12}$$

and can therefore be used as a basis in which more complex wave functions are expanded, provided they obey the same boundary conditions.

As shown in Figure 2.1 the energy spectrum of the ring consists of a set of translated parabolas and is periodic in the magnetic flux. This periodicity of the spectrum is related to the Aharonov-Bohm effect [10] (for a good review see [83]). At zero magnetic field there exists a left/right symmetry in the system, there is no preferred direction of motion. The magnetic field breaks this symmetry and lifts the degeneracies of the spectrum. The negative angular momentum states ($m > 0$) are lowered in energy with increasing magnetic flux since in this direction of motion the orbital magnetic moment of the electrons is aligned with the direction of the field. The ground state moves to higher angular momentum states as the flux grows in order to minimize the effective kinetic energy of the electrons. However, there are values of the flux at which the magnetic field does not manage to break the left/right symmetry and the spectrum becomes degenerate again, but in different pairs than those at $B = 0$.

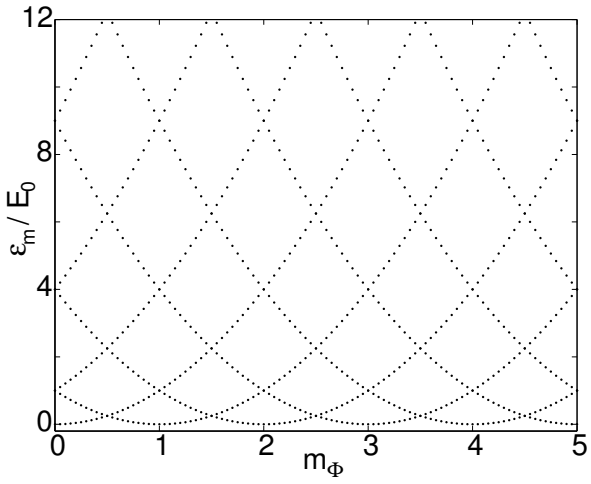

Figure 2.1: *Single-particle energy spectrum ϵ_m of the one-dimensional ring as a function of the magnetic flux.*

2.2 The Density Matrix

To fully specify the state of a many-electron system its state vector $|\Psi\rangle$, along with information about the occupation of single-electron states, must be known. The relevant physical properties are extracted by the expectation value of the representative operator

$$\left\langle \hat{A} \right\rangle = \langle \Psi | \, \hat{A} \, | \Psi \rangle \, . \tag{2.13}$$

There is another way to specify the state of the system which incorporates information about the occupation of single-electron states, namely the density matrix. The density matrix formalism has a clear advantage when inspecting a system subject to a nonadiabatic perturbation. Under these conditions the system is not in equilibrium at each time instant and the concepts of single-electron energy levels and their occupation is ill-defined in the sense that the stationary Schrödinger equation has no meaning at each time step. The time evolution of this information is included in the density matrix at all times. Furthermore, the representation of the equations of motion in terms of the density matrix often serves to simplify them.

In equilibrium we assume that the many-body state of a system can be described by a set of single-particle states which are solutions to the stationary Schrödinger equation

$$\hat{H} \, |\psi_i\rangle = \varepsilon_i \, |\psi_i\rangle \, , \tag{2.14}$$

where $\hat{H}$ is the Hamiltonian of the system. The probability that eigenstate i of the system is occupied at temperature T is given by the Fermi distribution

$$f_i = f(\varepsilon_i - \mu) = \frac{1}{1 + \exp\left(\frac{\varepsilon_i - \mu}{k_B T}\right)}, \tag{2.15}$$

where k_B is the Boltzmann constant and μ the chemical potential which is fixed by the number of electrons

$$\sum_{i=1}^{\infty} f_i = N_e. \tag{2.16}$$

The density operator of the system is defined as

$$\hat{\rho} = \sum_i f_i \left|\psi_i\right\rangle \left\langle\psi_i\right| \tag{2.17}$$

and by expanding the eigenstates of the Hamiltonian in the complete orthonormal basis (2.10)

$$\left|\psi_i\right\rangle = \sum_m c_{im} \left|m\right\rangle \tag{2.18}$$

the elements of the ground state density matrix with respect to this basis become

$$\begin{aligned} \rho_{lm} &= \left\langle l \right| \hat{\rho} \left|m\right\rangle \\ &= \sum_i f_i \sum_{n,n'} c^*_{in'} c_{in} \left\langle l \right| n\rangle \left\langle n'\right|m\rangle \\ &= \sum_i f_i \, c^*_{im} \, c_{il}, \end{aligned} \tag{2.19}$$

where in the second step we have used the orthonormality of the basis.

The density matrix fully characterizes the quantum state of a system. The expectation value of an operator $\hat{A}$ is given by

$$\left\langle \hat{A} \right\rangle = \mathrm{Tr}\{\hat{\rho}\hat{A}\} \tag{2.20}$$

so e.g. the electron density is found by

$$\begin{aligned} n(\mathbf{r}) &= \langle \delta(\hat{\mathbf{r}} - \mathbf{r}) \rangle = \mathrm{Tr}\{\hat{\rho}\,\delta(\hat{\mathbf{r}} - \mathbf{r})\} = \sum_l \langle\, l \,|\, \hat{\rho}\,\delta(\hat{\mathbf{r}} - \mathbf{r}) \,|\, l \,\rangle \\ &= \sum_l \int d\mathbf{r}' \,\langle\, l \,|\, \hat{\rho} \,|\mathbf{r}'\rangle \,\langle \mathbf{r}'|\, \delta(\hat{\mathbf{r}} - \mathbf{r}) \,|\, l \,\rangle \\ &= \sum_l \int d\mathbf{r}' \,\langle\, l \,|\, \hat{\rho} \,|\mathbf{r}'\rangle \,\langle \mathbf{r}'|\, \delta(\mathbf{r}' - \mathbf{r}) \,|\, l \,\rangle \\ &= \sum_{l,m} \int d\mathbf{r}' \delta(\mathbf{r}' - \mathbf{r}) \,\langle\, l \,|\, \hat{\rho} \,|m\rangle \,\langle m|\mathbf{r}'\rangle \,\langle \mathbf{r}'|\, l \,\rangle \\ &= \sum_{l,m} \int d\mathbf{r}' \delta(\mathbf{r}' - \mathbf{r}) \rho_{lm} \phi_m^*(\mathbf{r}') \phi_l(\mathbf{r}') \\ &= \sum_{l,m} \rho_{lm} \phi_m^*(\mathbf{r}) \phi_l(\mathbf{r}). \end{aligned} \tag{2.21}$$

Furthermore the density matrix obeys the constraint

$$\mathrm{Tr}\{\hat{\rho}\} = \sum_l \rho_{ll} = N_e, \tag{2.22}$$

where N_e is the number of electrons.

2.3 The Interacting Many-electron System

For an accurate description of a quantum system the Coulomb repulsion between electrons must be included. In one-dimensional systems the Coulomb interaction exhibits a bad singularity and its consequences are not fully known, although attempts towards an exact description have been made, in particular with the Luttinger liquid model [84]. To eliminate the singularity the Couloumb repulsion is here represented by a screened interaction and the role of the screening is investigated.

Due to the Coulomb interaction, the many-electron Schrödinger equation becomes too complex to solve directly except for few-electron systems. Therefore we will make use of the Hartree-Fock approximation, the main topic of the following sections.

2.3.1 The Hartree-Fock Approximation

The Hamiltonian of an N_e-electron system in a magnetic field described by the vector potential $\mathbf{A}$ is given by

$$H = \sum_{i=1}^{N_e} \frac{1}{2m^*} \left(\mathbf{p}_i + e\mathbf{A}\right)^2 + \frac{g^*\mu_B}{\hbar} \sum_{i=1}^{N_e} \mathbf{B} \cdot \mathbf{S}_i + H_{\mathrm{ext}} + \frac{1}{2} \sum_{i \neq j=1}^{N_e} \frac{e^2}{4\pi\epsilon_0\epsilon_r \left|\mathbf{r}_i - \mathbf{r}_j\right|}, \tag{2.23}$$

where the first term is the effective kinetic energy followed by the Zeeman term which represents the interaction of the spin of the electrons with the external magnetic field. External effects, e.g. background potentials and perturbations, are included in H_{ext} and the last term is the Coulomb repulsion between the electrons. The many-electron wave function of the system

$$\langle \mathbf{x}|\Psi\rangle = \Psi(\mathbf{r}_1 s_1, \mathbf{r}_2 s_2, \ldots, \mathbf{r}_{N_e} s_{N_e}), \tag{2.24}$$

which is a function of the spatial and spin coordinates ($\mathbf{x}_i = (\mathbf{r}_i s_i)$) of all electrons in the system, is a solution of the Schrödinger equation

$$\hat{H}\,|\Psi\rangle = E\,|\Psi\rangle\,. \tag{2.25}$$

Except for systems containing very few electrons, solving the many-body Schrödinger equation numerically is practically an impossible task even on todays powerful computers. This is mainly due to the Coulomb interaction and symmetry requirements on the wave function. Therefore some approximations have to be made. Several methods have been devised to solve the many-body Schrödinger equation and one of those is the Hartree-Fock method which will be presented here.

Electrons are identical particles, therefore, when interchanging the coordinates of two electrons, i and j, the physical predictions have to remain the same, i.e. the charge density $|\Psi|^2$ must not change. On interchanging a pair of electrons twice, the wave function does not change. Therefore,

$$\Psi(\mathbf{x}_1, \mathbf{x}_2, \ldots, \mathbf{x}_i, \ldots, \mathbf{x}_j, \ldots, \mathbf{x}_{N_e}) = \pm\Psi(\mathbf{x}_1, \mathbf{x}_2, \ldots, \mathbf{x}_j, \ldots, \mathbf{x}_i, \ldots, \mathbf{x}_{N_e}). \tag{2.26}$$

The wave function of a system of electrons, and all other Fermions, is antisymmetric with respect to particle exchange and so the minus sign applies in (2.26). The antisymmetry of the wave function leads to the Pauli principle, which states that only one electron may occupy a particular state. The simplest antisymmetric wave functions which can be used to construct an approximation of the state of a system of electrons are Slater determinants. In the Hartree Fock method the many-electron wave function is assumed to be represented by a single Slater determinant of a set of orthonormal spin orbitals $\{\chi_i\}$

$$\begin{aligned}\Psi &= \frac{1}{\sqrt{N_e!}}\det\{\chi_i(\mathbf{r}_j s_j)\} \\ &= \frac{1}{\sqrt{N_e!}}\begin{vmatrix} \chi_1(\mathbf{r}_1 s_1) & \chi_1(\mathbf{r}_2 s_2) & \ldots & \chi_1(\mathbf{r}_{N_e} s_{N_e}) \\ \chi_2(\mathbf{r}_1 s_1) & \chi_2(\mathbf{r}_2 s_2) & \ldots & \chi_2(\mathbf{r}_{N_e} s_{N_e}) \\ \vdots & \vdots & & \vdots \\ \chi_{N_e}(\mathbf{r}_1 s_1) & \chi_{N_e}(\mathbf{r}_2 s_2) & \ldots & \chi_{N_e}(\mathbf{r}_{N_e} s_{N_e}) \end{vmatrix}.\end{aligned} \tag{2.27}$$

It depicts a system of N_e electrons occupying N_e spin orbitals, without specifying in which orbital each electron resides. An important choice lies in the set of spin orbitals used to construct the Slater determinant as it should be the best approximation to the ground state of the system described by $\hat{H}$. This is achieved by varying the spin orbitals until the total electronic energy $E = \langle\Psi|\,\hat{H}\,|\Psi\rangle$ is at minimimum. This procedure leads to a nonlocal single-particle eigenvalue equation, the Hartree-Fock equation [85, 86]

$$\hat{\mathcal{F}}\,|\chi_i\rangle = \varepsilon_i\,|\chi_i\rangle\,, \tag{2.28}$$

where the Fock operator $\hat{\mathcal{F}}$ is given by

$$\begin{aligned}\mathcal{F}\chi_i(\mathbf{x}) = \left[h_0 + \frac{1}{2}g^*\mu_B B\sigma_z + H_{\text{ext}}\right]\chi_i(\mathbf{x}) + \frac{e^2}{4\pi\epsilon_0\epsilon_r}\sum_{j=1}^{N_e}\Bigg[\\ \int d\mathbf{x}'\;|\chi_j(\mathbf{x}')|^2\,\frac{1}{|\mathbf{r}-\mathbf{r}'|}\chi_i(\mathbf{x}) + \int d\mathbf{x}'\,\chi_j^*(\mathbf{x}')\frac{1}{|\mathbf{r}-\mathbf{r}'|}\chi_i(\mathbf{x}')\chi_j(\mathbf{x})\Bigg].\end{aligned} \tag{2.29}$$

The term within square brackets is the single-particle part of the Hamiltonian, where the spin has been restricted to the z direction, with $\sigma_z = \pm 1$. The two following terms represent the Coulomb interaction between electrons in an averaged way. The first is the direct or Hartree term

$$J_i(\mathbf{x}) = \int d\mathbf{x}'\;|\chi_i(\mathbf{x}')|^2\,|\mathbf{r}-\mathbf{r}'|^{-1}\,. \tag{2.30}$$

It is the classical Coulomb repulsion that an electron feels due to electron i and in summing over i the electrostatic energy of the electron in the presence of the charge distribution is obtained. The second is called the exchange term and is nonlocal in contrast to the Hartree potential. It appears because of the antisymmetry requirement on the wave function. The exchange operator $K_i(\mathbf{x})$ is determined by its effect on the wave function it operates on

$$K_i(\mathbf{x})\psi(\mathbf{x}) = \int d\mathbf{x}'\,\chi_i^*(\mathbf{x}')\,|\mathbf{r}-\mathbf{r}'|^{-1}\,\psi(\mathbf{x}')\chi_i(\mathbf{x}). \tag{2.31}$$

When operating on a function $\psi(\mathbf{x})$ the exchange potential depends on the value of the function throughout space, i.e. there doesn't exist a potential $K_i(\mathbf{x})$ which is uniquely defined at any point in space. The exchange term is nonzero only for electrons of the same spin, making their motion correlated. In the Hartree-Fock method correlations between electrons of opposite spin are neglected. Using (2.30) and (2.31) the Fock

operator can be written

$$\begin{aligned}\mathcal{F}(\mathbf{x}) &= h_0 + \frac{1}{2}g^*\mu_B B\sigma_z + H_{\text{ext}} + \frac{e^2}{4\pi\epsilon_0\epsilon_r}\sum_{i=1}^{N_e}\left[J_i(\mathbf{x}) - K_i(\mathbf{x})\right] \\ &= h + \frac{e^2}{4\pi\epsilon_0\epsilon_r}\sum_{i=1}^{N_e}\left[J_i(\mathbf{x}) - K_i(\mathbf{x})\right].\end{aligned} \tag{2.32}$$

The Hartree-Fock method reduces the many-electron problem to a set of single-particle eigenvalue equations by approximating the Coulomb interaction as an average nonlocal potential field created by all electrons in the system. Although the problem has been greatly simplified, the interaction terms depend on the spin orbitals which are solutions of the Hartree-Fock equation. Before elaborating the method of solution the choice of spin orbitals will be worked further resulting in the unrestricted Hartree-Fock method.

2.3.2 Unrestricted Hartree-Fock Method

To derive an expression of the Hartree-Fock equation convenient for numerical evaluation the form of the spin orbitals must be specified. The form used here leads to the Pople-Nesbet equations [87] in which the density matrix plays a leading role.

The spin orbitals used to construct the Slater determinant are assumed to be a product of a spatial orbital and a spin function

$$\chi_i(\mathbf{r}s) = \begin{cases}\psi_j^\alpha(\mathbf{r})\alpha(s) \\ \psi_j^\beta(\mathbf{r})\beta(s)\end{cases} \tag{2.33}$$

and the spatial orbitals are not restricted to the same form for the two spin directions. The sets $\{\psi_j^\alpha\}$ and $\{\psi_j^\beta\}$ individually form orthonormal sets. However, members of $\{\psi_j^\alpha\}$ are not necessarily orthogonal to members of $\{\psi_j^\beta\}$. The set of spin orbitals $\{\chi_i\}$ still forms an orthonormal set, either from spatial or spin orthogonality

$$\langle\alpha|\beta\rangle = \int ds\, \alpha^*(s)\beta(s) = \delta_{\alpha\beta}. \tag{2.34}$$

Inserting (2.33) into the Hartree-Fock equation (2.28) gives

$$\begin{aligned}\mathcal{F}\psi_j^\alpha(\mathbf{r})\alpha(s) &= \varepsilon_j^\alpha\psi_j^\alpha(\mathbf{r})\alpha(s) \\ \mathcal{F}\psi_j^\beta(\mathbf{r})\beta(s) &= \varepsilon_j^\beta\psi_j^\beta(\mathbf{r})\beta(s),\end{aligned} \tag{2.35}$$

where the eigenenergies ε_j^α and ε_j^β are not necessarily the same. Multiplying (2.35) by $\alpha^*(s)$ and $\beta^*(s)$ respectively and integrating over spin leads to

$$\begin{aligned} \mathcal{F}^\alpha(\mathbf{r})\psi_j^\alpha(\mathbf{r}) &= \varepsilon_j^\alpha \psi_j^\alpha(\mathbf{r}) \\ \mathcal{F}^\beta(\mathbf{r})\psi_j^\beta(\mathbf{r}) &= \varepsilon_j^\beta \psi_j^\beta(\mathbf{r}), \end{aligned} \tag{2.36}$$

with the spatial Fock operators given by

$$\begin{aligned} \mathcal{F}^\alpha(\mathbf{r}) &= \int ds\, \alpha^*(s)\mathcal{F}(\mathbf{r},s)\alpha(s) \\ \mathcal{F}^\beta(\mathbf{r}) &= \int ds\, \beta^*(s)\mathcal{F}(\mathbf{r},s)\beta(s). \end{aligned} \tag{2.37}$$

From now on we will only show the equations for spin α, to obtain the analogous expressions for spin β simply replace α by β and vice versa. Performing the integration in (2.37) it can be shown that the spatial Fock operator will include the single-electron operator $\hat{h}$, direct interaction with all electrons of the system, as well as the exchange interaction with electrons of the same spin. Thus

$$\hat{\mathcal{F}}^\alpha = \hat{h} + \frac{e^2}{4\pi\epsilon_0\epsilon_r}\sum_i^{N_e^\alpha}\left[\hat{J}_i^\alpha - \hat{K}_i^\alpha\right] + \frac{e^2}{4\pi\epsilon_0\epsilon_r}\sum_i^{N_e^\beta}\hat{J}_i^\beta, \tag{2.38}$$

where $\hat{J}$ is the spatial Coulomb operator

$$J_i^\alpha(\mathbf{r}) = \int d\mathbf{r}'\, |\psi_i^\alpha(\mathbf{r}')|^2\, |\mathbf{r}-\mathbf{r}'|^{-1} \tag{2.39}$$

and $\hat{K}$ the spatial exchange operator

$$K_i^\alpha(\mathbf{r})\psi_j^\alpha(\mathbf{r}) = \left[\int d\mathbf{r}'\psi_i^{\alpha*}(\mathbf{r}')\, |\mathbf{r}-\mathbf{r}'|^{-1}\, \psi_j^\alpha(\mathbf{r}')\right]\psi_i^\alpha(\mathbf{r}). \tag{2.40}$$

The sum over the N_e^α orbitals ψ_i^α in (2.38) formally includes the interaction of an α-electron with itself. However, since

$$\left[\hat{J}_i^\alpha - \hat{K}_i^\alpha\right]|\psi_i^\alpha\rangle = 0, \tag{2.41}$$

this self-interaction is eliminated.

To solve the two eigenvalue equations (2.36) the spatial orbitals are expanded in a complete orthonormal basis $\{\phi_m\}$ (here the basis of $\hat{h}_0$ (2.10) is used).

$$\left|\psi_j^\alpha\right\rangle = \sum_{m=-\infty}^{\infty} c_{jm}^\alpha \left|\phi_m\right\rangle. \tag{2.42}$$

Substituting the expansion (2.42) into (2.36) the Hartree-Fock equation becomes

$$\sum_m c_{jm}^\alpha \hat{\mathcal{F}}^\alpha |\phi_m\rangle = \varepsilon_j^\alpha \sum_m c_{jm}^\alpha |\phi_m\rangle \tag{2.43}$$

and projecting it onto $\langle\phi_l|$ gives a matrix eigenvalue equation, the Pople-Nesbet equation [87]

$$\sum_m \mathcal{F}_{lm}^\alpha c_{jm}^\alpha = \varepsilon_j^\alpha \sum_m c_{jm}^\alpha \langle\phi_l|\phi_m\rangle = \varepsilon_j^\alpha c_{jl}^\alpha, \tag{2.44}$$

where

$$\mathcal{F}_{lm}^\alpha = \langle\phi_l| \hat{\mathcal{F}}^\alpha |\phi_m\rangle = \int d\mathbf{r}\, \phi_l^*(\mathbf{r}) \mathcal{F}^\alpha(\mathbf{r}) \phi_m(\mathbf{r}). \tag{2.45}$$

To find the matrix representation of the Fock matrix $\mathcal{F}_{lm}^\alpha$ in terms of the density matrix we insert the Fock operator (2.38) into (2.45)

$$\begin{aligned}
\mathcal{F}_{lm}^\alpha &= h_{lm} + \frac{e^2}{4\pi\epsilon_0\epsilon_r} \sum_i^{N_e^\alpha} \int d\mathbf{r}\, \phi_l^*(\mathbf{r}) \left[J_i^\alpha(\mathbf{r}) - K_i^\alpha(\mathbf{r})\right] \phi_m(\mathbf{r}) \\
&\qquad + \frac{e^2}{4\pi\epsilon_0\epsilon_r} \sum_i^{N_e^\beta} \int d\mathbf{r}\, \phi_l^*(\mathbf{r}) J_i^\beta(\mathbf{r}) \phi_m(\mathbf{r}) \\
&= h_{lm} + \frac{e^2}{4\pi\epsilon_0\epsilon_r} \sum_i^{N_e^\alpha} \int d\mathbf{r}\, d\mathbf{r}' \Big[\phi_l^*(\mathbf{r}) \psi_i^{\alpha*}(\mathbf{r}') |\mathbf{r}-\mathbf{r}'|^{-1} \psi_i^\alpha(\mathbf{r}') \phi_m(\mathbf{r}) \\
&\qquad - \phi_l^*(\mathbf{r}) \psi_i^{\alpha*}(\mathbf{r}') |\mathbf{r}-\mathbf{r}'|^{-1} \phi_m(\mathbf{r}') \psi_i^\alpha(\mathbf{r})\Big] \\
&\quad + \frac{e^2}{4\pi\epsilon_0\epsilon_r} \sum_i^{N_e^\beta} \int d\mathbf{r}\, d\mathbf{r}'\, \phi_l^*(\mathbf{r}) \psi_i^{\beta*}(\mathbf{r}') |\mathbf{r}-\mathbf{r}'|^{-1} \psi_i^\beta(\mathbf{r}') \phi_m(\mathbf{r})
\end{aligned} \tag{2.46}$$

and with the expansion (2.42) we obtain

$$\begin{aligned}
\mathcal{F}_{lm}^\alpha =& h_{lm} + \frac{e^2}{4\pi\epsilon_0\epsilon_r} \sum_{n,p} \Bigg[\sum_i^{N_e^\alpha} c_{in}^{\alpha*} c_{ip}^\alpha \int d\mathbf{r}\, d\mathbf{r}' \\
&\Big[\phi_l^*(\mathbf{r}) \phi_n^*(\mathbf{r}') |\mathbf{r}-\mathbf{r}'|^{-1} \phi_p(\mathbf{r}') \phi_m(\mathbf{r}) - \phi_l^*(\mathbf{r}) \phi_n^*(\mathbf{r}') |\mathbf{r}-\mathbf{r}'|^{-1} \phi_m(\mathbf{r}') \phi_p(\mathbf{r})\Big] \\
&+ \sum_i^{N_e^\beta} c_{in}^{\beta*} c_{ip}^\beta \int d\mathbf{r}\, d\mathbf{r}'\, \phi_l^*(\mathbf{r}) \phi_n^*(\mathbf{r}') |\mathbf{r}-\mathbf{r}'|^{-1} \phi_p(\mathbf{r}') \phi_m(\mathbf{r}) \Bigg].
\end{aligned} \tag{2.47}$$

When the temperature is finite the Fermi distribution (2.15) is included in the sum over i. Using the definition of the density matrix (2.19) for each spin direction as well as the shorthand notation

$$\langle\psi_i\psi_j|\psi_k\psi_l\rangle = \int d\mathbf{r}\, d\mathbf{r}'\, \psi_i^*(\mathbf{r}) \psi_j^*(\mathbf{r}') |\mathbf{r}-\mathbf{r}'|^{-1} \psi_k(\mathbf{r}) \psi_l(\mathbf{r}'), \tag{2.48}$$

the Fock matrix can be written

$$\begin{aligned}\mathcal{F}^{\alpha}_{lm} &= h_{lm} + \frac{e^2}{4\pi\epsilon_0\epsilon_r}\sum_{n,p} \\ &\qquad \left[\sum_{i}^{N_e^{\alpha}} f_i c^{\alpha *}_{in} c^{\alpha}_{ip}\Big[\langle\phi_l\phi_n|\phi_m\phi_p\rangle - \langle\phi_l\phi_n|\phi_p\phi_m\rangle\Big] + \sum_{i}^{N_e^{\beta}} f_i c^{\alpha *}_{in} c^{\alpha}_{ip}\langle\phi_l\phi_n|\phi_m\phi_p\rangle\right] \\ &= h_{lm} + \frac{e^2}{4\pi\epsilon_0\epsilon_r}\sum_{n,p}\Big[\rho^{\alpha}_{pn}\big[\langle\phi_l\phi_n|\phi_m\phi_p\rangle - \langle\phi_l\phi_n|\phi_p\phi_m\rangle\big] + \rho^{\beta}_{pn}\langle\phi_l\phi_n|\phi_m\phi_p\rangle\Big] \\ &= h_{lm} + \frac{e^2}{4\pi\epsilon_0\epsilon_r}\sum_{n,p}\Big[\rho^{T}_{pn}\langle\phi_l\phi_n|\phi_m\phi_p\rangle - \rho^{\alpha}_{pn}\langle\phi_l\phi_n|\phi_p\phi_m\rangle\Big],\end{aligned} \tag{2.49}$$

where ρ^T is the total density matrix

$$\rho^T = \rho^{\alpha} + \rho^{\beta}. \tag{2.50}$$

2.3.3 SOLVING THE HF-EQUATIONS

The Hartree-Fock equations (2.36) are nonlinear integro-differential equations whose solutions are the occupied single-electron states $\psi^{\alpha}_j(\mathbf{r})$ and the corresponding energy levels. By expanding the unknown orbitals in a convenient basis the equations are converted into a nonlinear matrix eigenvalue equation

$$\mathbb{F}(\mathbf{c})\,\mathbf{c} = \varepsilon\,\mathbf{c} \tag{2.51}$$

where $\mathbf{c}$ are the expansion coefficients and ε a diagonal matrix containing the energy eigenvalues. Solving (2.51) directly is a hard task, since the Fock matrix (2.49) depends on the solution itself. A standard approach to solving (2.51) is in an iterative scheme, the so-called self-consistent field method. Initially a guess for the expansion coefficients, or equivalently the density matrix ρ, is used to construct the Fock matrix, thereby transforming the problem to a linear eigenvalue equation which can be solved by standard numerical methods. The solution is then used to construct a new estimate for ρ which is used as input for the Fock matrix. This procedure is repeated until the solution converges and self-consistency is achieved. The convergence criterion is that the change in a chosen parameter (the density matrix, total energy, etc.) from one iteration to the next is less than a prescribed tolerance value. In many cases, using the solution in each step directly in the Fock matrix leads to a convergence instability. To stabilize the convergence a common method is to only use the new solution partly,

i.e. to mix the new solution ρ_{sol} with the one from the previous step

$$\rho^n = x\rho_{\text{sol}} + (1-x)\rho^{n-1}, \tag{2.52}$$

where x is the mixing weight (often in the range of $x = 0.05 - 0.1$ or even smaller).

The Hartree-Fock equation is derived by using the variational principle, which states that by varying the spin orbitals such that the change in the total energy becomes zero, we may find the set of spin orbitals, for the Slater determinantal wave function, which minimize the total electronic energy. The Hartree-Fock equation is thus obtained as a condition that the energy reaches its minimum, which is an upper bound to the true ground state energy. However, this condition is only necessary, but *not sufficient*, for obtaining the ground state solution. The initial guess used to construct the Fock matrix as well as numerical errors can have a marked effect on the solution found by iteration. It is possible, and even quite common, that the solution persists in a local energy minimum which represents an excited state of the system. Normally, as an initial guess, the density matrix of the corresponding noninteracting system is used. To "scan" the energy landscape, the initial guess is slightly modified and the total energy of the resulting solutions are compared to determine which is the true ground state (or at least closest to it). For varying the initial guess we start the iterative procedure with a higher value of the Zeeman energy in order to lift the spin (semi) degeneracy of the spectrum. After a few iterations, the Zeeman energy is relaxed to its true value. A degenerate spectrum leads more easily to oscillations in the convergence, i.e. to a jump between two solutions during iteration.

To solve the matrix eigenvalue equation (2.44) the two-electron integrals (2.48), included in the interaction terms of the Fock matrix, have to be evaluated. The interaction is represented by a screened interaction along a straight line connecting two electrons at θ and θ',

$$|\mathbf{r} - \mathbf{r}'|^{-1} \to \left(r_0 \sqrt{\sin^2\left[(\theta - \theta')/2\right] + \mu_s^2} \right)^{-1}. \tag{2.53}$$

The screening parameter μ_s eliminates the singularity of the Coulomb interaction at $\theta = \theta'$. Normally, the two-electron integrals are calculated by numerical quadrature for a fixed screening constant. However, the plane-wave basis (2.10) permits an analytical calculation of the integrals making it possible to easily vary μ_s even in the limit of $\mu_s \to 0$. The two-electron integrals are thus found to be (see Appendix A for a detailed derivation)

$$\langle \phi_l \phi_n | \phi_m \phi_p \rangle = \frac{2}{\pi r_0} Q_{p-n-\frac{1}{2}}(2\mu_s^2 + 1)\, \delta_{l-m,p-n}, \quad l, m, n, p = 0, \pm 1, \pm 2, \ldots, \tag{2.54}$$

where $Q_\nu(x)$ is the Lagrange function of the second kind [88]. The asymptotic form of the Lagrange function is known in the vicinity of $x = 1^+$ (equivalent to $\mu_s \to 0$) and obeys a recursion relation in the indices. Having an analytical expression for the two-electron integrals greatly reduces the computational task of solving the Hartree-Fock equations.

2.3.4 Interacting Single-electron Spectrum

The solutions of the Hartree-Fock equation yield an approximation to the ground state of the quantum ring. The energy eigenvalues form a single-electron spectrum which gives information about e.g. the spin structure of the system as well as the influence of the Coulomb interaction. First we will look at the effect of the screening constant μ_s upon the spectrum and then choose a value of μ_s where the interaction is of similar magnitude as the kinetic energy of the electrons to see how the strength of the interaction affects the properties of the system. Following that the total electronic energy is discussed. The system is modeled in a GaAs semiconductor heterostructure at a temperature $T = 4$K with an effective electron mass $m^* = 0.067m$, where m is the free electron mass, and an effective g-factor $g^* = -0.44$. The ring has a radius of $r_0 = 14$ nm and contains up to 10 electrons.

In the case of a flat ring (no background potential), the Coulomb interaction is rotationally invariant and is therefore unable to couple states of different angular momentum due to the conservation of total angular momentum. Therefore, since the basis functions used are the eigenfunctions of the angular momentum operator, its matrix elements are diagonal. This fact can be used to derive an expression for the energy contribution of the interaction within the Hartree-Fock approximation (see Appendix B)

$$\begin{aligned} E_{\text{int}} = &-2N_e^\alpha N_e^\beta \left[\gamma + \ln\mu_s + \psi(\tfrac{1}{2})\right] - \psi(\tfrac{1}{2})\left[(N_e^\alpha)^2 + (N_e^\beta)^2\right] \\ &+ \sum_m \rho^\alpha_{mm} \sum_n \rho^\alpha_{nn}\, \psi(m-n+\tfrac{1}{2}) + \sum_m \rho^\beta_{mm} \sum_n \rho^\beta_{nn}\, \psi(m-n+\tfrac{1}{2}), \end{aligned} \tag{2.55}$$

which clarifies the effect of μ_s upon the ground state. Although the density matrices ρ^α and ρ^β are implicitly dependent on μ_s its primary influence, when it is small, is through the logarithmic term $\ln\mu_s$. A very small value of the screening constant contributes a large value to the interaction energy. Under those conditions it becomes energetically favourable for the system to spin polarize, i.e. only the lowermost N_e levels of one spin direction are occupied, and the $\ln\mu_s$ term disappears from (2.55). As μ_s increases its

contribution to the energy gradually diminishes as the influence of the kinetic energy grows and at some point it becomes unnecessary for the system to spin polarize

In the region where μ_s causes the system to spin polarize the spectrum is very similar to that of a noninteracting system (shown in Figure 2.1, page 8). In Figure 2.2 the spectrum of four electrons confined to the ring is shown for two small values of μ_s. The only discernible difference between the two cases is that when μ_s decreases the gap between the lowest levels of opposite spin directions, the spin split, becomes larger. As the screening parameter becomes smaller the interaction energy grows logarithmically and tends to infinity as $\mu_s \to 0$. The effect of the magnitude of μ_s on the occupied levels is negligible when μ_s is small. Therefore the physical properties of the system are unchanged and qualitatively similar to the predictions of a noninteracting model.

In a range around $\mu_s = 0.025$ the effective kinetic energy term, $\hat{h}_0$ (2.4), and the exchange term of the Hamiltonian compete for control over the system. This leads to a single-electron spectrum which is quite different from that of a noninteracting system. As shown in Figure 2.3 there is a difference in the spectrum depending on whether there is an odd or an even number of electrons on the ring. For 4 electrons the spectrum shifts between regions where the system is spin polarized, and only electrons of the same spin are present, and regions where the system contains an equal number of up and down spin electrons. When the system becomes spin polarized, the difference in kinetic energy between a spin polarized state and a spin degenerate one is not enough to balance the gain in exchange energy. Thus the properties of the system are a result of an interplay between kinetic energy and interaction. For fewer electrons the Coulomb interaction is the main source of influence. In this case the spectrum is fully spin polarized and is qualitatively similar to that of a noninteracting system. With increasing number of electrons the kinetic energy becomes the primary factor in the behaviour of the system. Therefore, for $N_e > 6$, the spectrum is spin degenerate (except for the Zeeman energy) and resembles that of a noninteracting model of the ring, in which the spin of the electrons is included. In the case of an odd number of electrons there is always some degree of spin splitting, since the number of electrons of opposite spin is unequal.

The total energy of the ring containing 3, 4 and 6 electrons is shown in Figure 2.4. In the case of an even large number of electrons the $S = 0$ state is the ground state at all values of the magnetic flux. As the number of electrons decreases and the importance of the Coulomb interaction increases, the $S = 1$ state comes down in energy and becomes the ground state for some values of m_Φ (eventually it is the

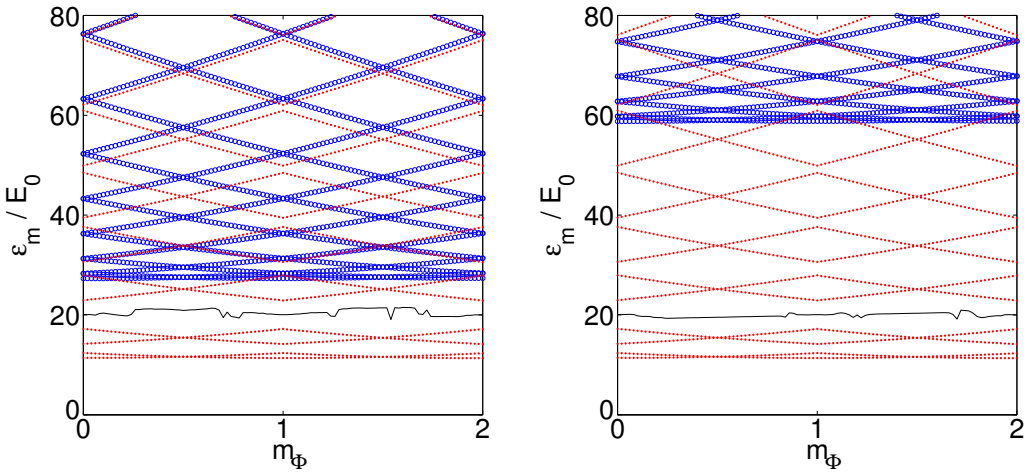

Figure 2.2: *Single-electron energy levels ε_m (in units of $E_0 = \hbar^2/2m^*r_0^2$) as a function of the external magnetic flux for 4 electrons on the ring. The screening constant is $\mu_s = 10^{-2}$ (left) and $\mu_s = 10^{-4}$ (right). Points and circles denote spin up ($\sigma_z = +1$) and spin down ($\sigma_z = -1$) states respectively. The solid line is the chemical potential.*

ground state at all values of the magnetic flux). This was observed by Niemelä et al. [63], the Coulomb interaction (or any kind of repulsive interaction) favors a spin $S = 1$ ground state. They suggest this is due to Hund's rule which states that the interaction energy is lower for a spatial wave function of lower symmetry. For the $S = 0$ state the spatial part of the wave function is symmetric with respect to particle exchange and thus it grows more in energy than the $S = 1$ state when interaction is included. For an odd number of electrons a strong Coulomb interaction favors a spin $S = \frac{3}{2}$ ground state and with increasing number of electrons the $S = \frac{1}{2}$ configuration becomes the ground state.

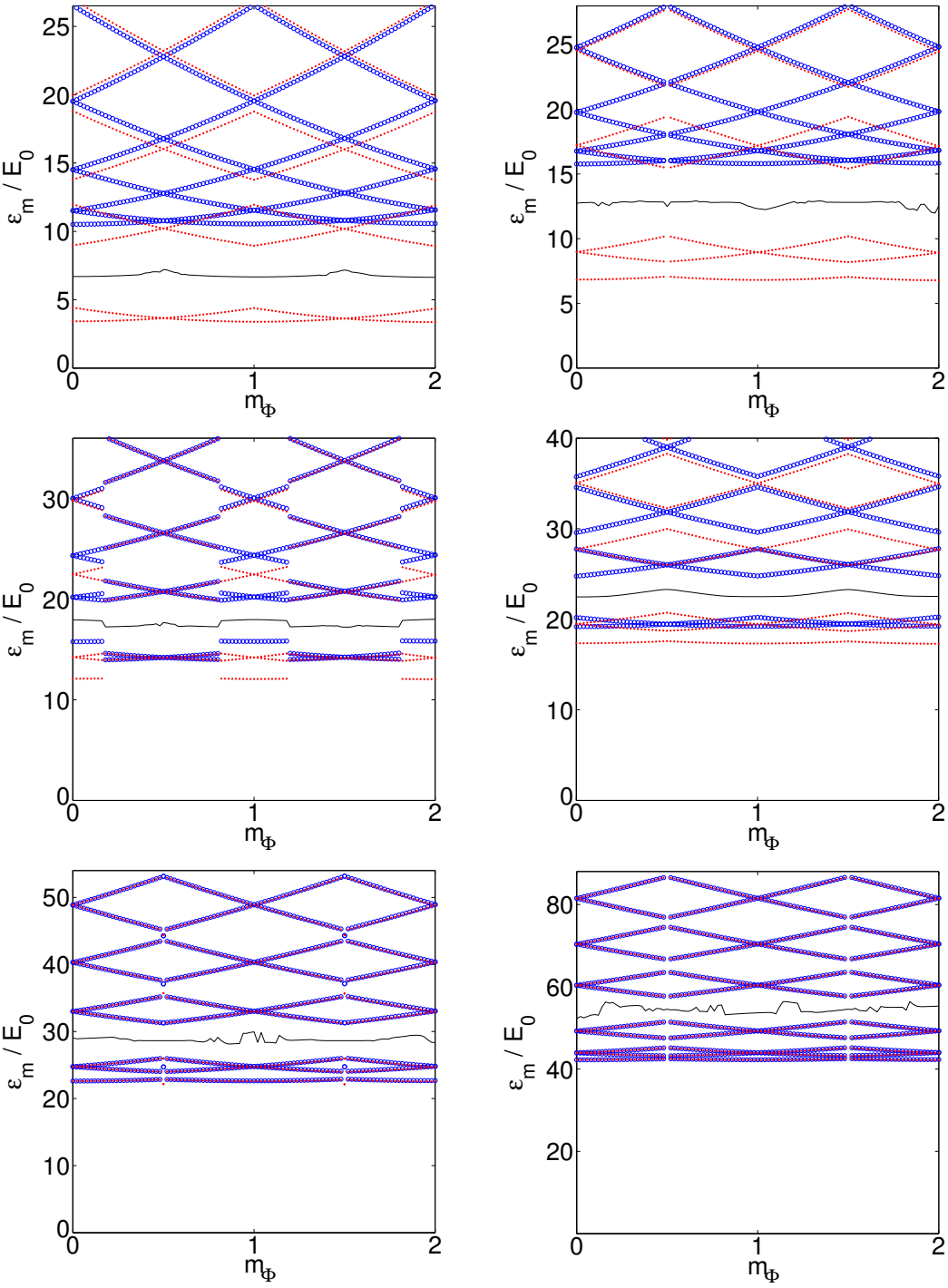

Figure 2.3: *Single-electron energy levels ε_m in units of $E_0 = \hbar^2/2m^*r_0^2$ as a function of the external magnetic flux for 2 (top left), 3 (top right), 4 (middle left), 5 (middle right), 6 (bottom left) and 10 (bottom right) interacting electrons within the Hartree-Fock approximation. The screening parameter is $\mu_s = 0.025$. Points and circles denote the energy of spin up and spin down electrons respectively, the solid line is the chemical potential.*

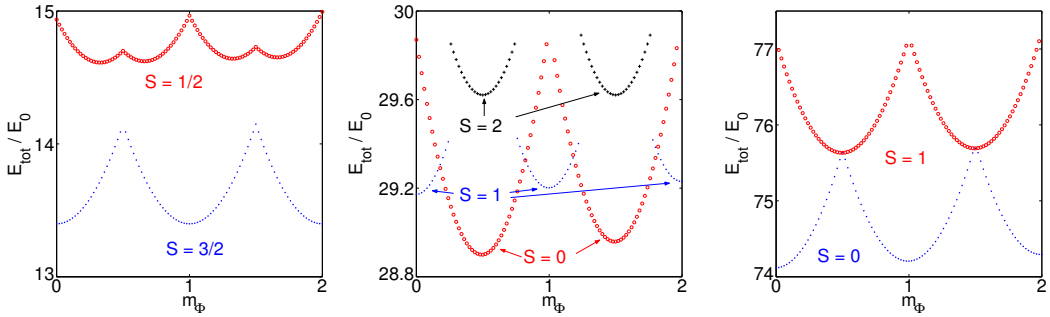

Figure 2.4: *Total electronic energy in units of* $E_0 = \hbar^2/2m^*r_0^2$ *as a function of the external magnetic flux for 3 (left), 4 (middle) and 6 (right) interacting electrons within the Hartree-Fock approximation. The screening parameter is* $\mu_s = 0.025$. *Points denote the groundstate energy and circles denote the energy of the first excited state.*

2.4 The Current on the Ring

The energy spectrum of the one-dimensional ring is periodic in the magnetic flux. This periodicity leads to an instrinsic property of the ring when placed in an external magnetic field, the persistent current. In section 3.4.1 the persistent current is discussed and following that, in section 3.4.2, its relation to the orbital magnetic moment of the system.

2.4.1 Persistent Current

The spectrum of the noninteracting one-dimensional ring is periodic in the magnetic flux with a period of Φ_0. By a gauge transformation the magnetic field can be eliminated from the Hamiltonian of the system resulting in a modification of the boundary condition such that

$$\phi(\theta + 2\pi) = \phi(\theta)e^{i2\pi\Phi/\Phi_0}, \tag{2.56}$$

the so called twisted boundary condition. This permits an analogy to be drawn between the quantum ring and an infinite periodic lattice in one dimension [6], where the unit cell is the circumference of the ring L and the Bloch wave vector is

$$k_l = \frac{2\pi}{L}\frac{\Phi}{\Phi_0}. \tag{2.57}$$

This analogy leads us to an interesting phenomenon manifested in the ring, the persistent current. The velocity of an electron in the l^{th} state is

$$v_l = \frac{1}{\hbar}\frac{\partial\varepsilon_l}{\partial k_l} = \frac{L}{e}\frac{\partial\varepsilon_l}{\partial\Phi} \tag{2.58}$$

and associated with that state is therefore an equilibrium current

$$I_l = -\frac{ev_l}{L} = -\frac{\partial \varepsilon_l}{\partial \Phi}. \tag{2.59}$$

The current is proportional to the slope of the energy band and is therefore also periodic in Φ. The total current encircling the ring is a sum of the currents of each occupied state, weighted by the occupation number

$$I_{\text{p.c.}} = \sum_l f(\varepsilon_l)\, I_l = -\sum_l f(\varepsilon_l) \frac{\partial \varepsilon_l}{\partial \Phi}. \tag{2.60}$$

Due to the monotonic increase of I_l with l and the near cancellation between pairs of filled bands the direction of the current is determined by the highest occupied state. The persistent current is not a transport current since no external influence is needed, it is an equilibrium property of the ring.

The persistent current appears because the external magnetic field breaks the left/right symmetry of the ring. At a zero magnetic field the occupation of states with equal but opposite direction of motion, $|m\rangle$ and $|-m\rangle$, is identical and the currents associated with the states therefore cancel each other. When the ring is placed in a magnetic field the states with negative angular momentum are lowered in energy with respect to the positive ones and their occupation consequently increases. Therefore a net, constant current appears.

2.4.2 Orbital Magnetic Moment

The orbital magnetic moment of a system is defined as[1] [89]

$$M_o = \frac{1}{2} \int d\mathbf{r} \left(\mathbf{r} \times \langle \mathbf{J}(\mathbf{r}) \rangle \right) \cdot \hat{\mathbf{n}}, \tag{2.61}$$

where $\hat{\mathbf{n}}$ is a unit vector perpendicular to the plane of the system and $\langle \mathbf{J}(\mathbf{r}) \rangle$ is the current density, averaged over the Fermi distribution (2.15). The current density can be derived from the continuity relation by assuming a Hamiltonian of the form

$$H = \frac{\mathbf{p}^2}{2m} + V(\mathbf{r}) \tag{2.62}$$

and is given by

$$\mathbf{J}(\mathbf{r}) = -\frac{e}{2} \big(\mathbf{v} \, |\mathbf{r}\rangle \, \langle \mathbf{r}| + |\mathbf{r}\rangle \, \langle \mathbf{r}| \, \mathbf{v} \big), \tag{2.63}$$

[1] In the literature this is commonly referred to as the magnetization.

where $\mathbf{v}$ is the effective velocity

$$\mathbf{v} = \frac{1}{m^*}\left(\mathbf{p} + e\mathbf{A}\right). \tag{2.64}$$

The orbital magnetic moment of a system of noninteracting electrons on a ring can be calculated by (2.61) (for a detailed derivation see Appendix C)

$$M_o = \mu_B^* \sum_m (m - m_\Phi)\rho_{mm}. \tag{2.65}$$

The Fock operator is not of the form (2.62) due to the nonlocality of the exchange potential. Therefore the orbital magnetic moment must be found differently. It is given by a sum of the magnetic moments of each single-electron state, weighted by the occupation number

$$M_o = \sum_i f_i \left\langle \psi_i \right| \hat{M}_o \left| \psi_i \right\rangle. \tag{2.66}$$

By expanding the spatial orbitals $|\psi_i\rangle$ in the basis (2.10),

$$\left|\psi_i\right\rangle = \sum_m c_{im} \left|m\right\rangle, \tag{2.67}$$

the orbital magnetic moment can be written

$$\begin{aligned} M_o &= \sum_{l,m}\sum_i f_i c_{il}^* c_{im} \left\langle l \right| \hat{M}_o \left| m \right\rangle \\ &= \sum_{l,m} \rho_{ml} \left\langle l \right| \hat{M}_o \left| m \right\rangle, \end{aligned} \tag{2.68}$$

where we have used the definition of the density matrix (2.19). The magnetic moment operator $\hat{M}_o$ is given by

$$\hat{M}_o = \frac{1}{2}\mathbf{r} \times \mathbf{j} = \frac{1}{2}(x j_y - y j_x), \tag{2.69}$$

where the current $\mathbf{j}$ is defined[2] as

$$\mathbf{j} = -e\dot{\mathbf{r}} = -\frac{ie}{\hbar}[H, \mathbf{r}] \quad \Rightarrow \quad \begin{aligned} j_x &= -\frac{ie}{\hbar}(Hx - xH) \\ j_y &= -\frac{ie}{\hbar}(Hy - yH). \end{aligned} \tag{2.70}$$

[2]The current is traditionally defined as $\mathbf{j} = -en\dot{\mathbf{r}}$, where n is the particle density. In the one-dimensional ring, omitting n results in the current per electron.

The Hartree-Fock current is nonlocal due to the exchange term in the Hamiltonian and therefore we can only evaluate its matrix elements explicitly. Using the completeness of the basis $\{|m\rangle\}$ the magnetic moment can be written

$$\begin{aligned} M_o = -\frac{ie}{2\hbar} \sum_{l,m,n,p} \rho_{ml} \Big[\langle l \,|\, x \,|n\rangle \Big(\langle n| \,\hat{H}\, |p\rangle \,\langle p|\, y \,|m\rangle - \langle n|\, y \,|p\rangle \,\langle p|\, \hat{H} \,|m\rangle \Big) \\ - \langle l \,|\, y \,|n\rangle \Big(\langle n| \,\hat{H}\, |p\rangle \,\langle p|\, x \,|m\rangle - \langle n|\, x \,|p\rangle \,\langle p|\, \hat{H} \,|m\rangle \Big) \Big] \qquad (2.71) \\ = -\frac{ie}{2\hbar} \sum_{l,m,n,p} \rho_{ml} \Big[x_{ln}(H_{np} y_{pm} - y_{np} H_{pm}) - y_{ln}(H_{np} x_{pm} - x_{np} H_{pm}) \Big]. \end{aligned}$$

Inserting for the matrix elements of x and y and simplifying the magnetic moment becomes

$$M_o = \frac{\mu_B^*}{4E_0} \left[\sum_{l,m=-N}^{N-1} \left(\rho_{ml} H_{l+1,m+1} - \rho_{m+1,l+1} H_{lm} \right) + \sum_{m=-N}^{N} \left(\rho_{mN} H_{Nm} - \rho_{m1} H_{1m} \right) \right]. \qquad (2.72)$$

For the noninteracting system it can be shown that (2.71) gives the same result as (2.65) for an infinite basis ($N \to \infty$). In practice the basis used has to be finite and this leads to a negligible cutoff error, if the basis is large enough.

The magnetic moment will in the following be used as a convenient measure of the persistent current on the ring, since the current is directly proportional to the it. Using the definitions

$$\mathbf{r} = r_0 \hat{e}_r \,, \qquad \mathbf{j} = \pm j \hat{e}_\theta, \qquad (2.73)$$

the magnetic moment can be written

$$M_o = \pm \frac{r_0 j}{2} \hat{e}_r \times \hat{e}_\theta = \pm \frac{r_0 j}{2} \hat{e}_z. \qquad (2.74)$$

Therefore the magnitude of the current is

$$j = \frac{2}{r_0} M_o = \frac{e\hbar}{m^* r_0} \frac{M_o}{\mu_B^*} \qquad (2.75)$$

and it has the same sign.

The ground state magnetic moment of the noninteracting quantum ring is shown in Figure 2.5 for 2-6 and 10 electrons. It is a periodic function of the magnetic flux with a period of Φ_0, a consequence of the periodicity of the energy spectrum. At integer and half-integer values of the magnetic flux the magnetic field cannot break the left/right symmetry of the system and the energy spectrum becomes degenerate. At these points the occupation of crossing levels is equal and the current they carry is

equal but in opposite direction. Therefore the persistent current disappears. For an even to odd number of electrons the current shifts from paramagnetic to diamagnetic, or opposite, since the slope of consecutive energy levels has the opposite sign.

When the screening constant μ_s is small the energy spectrum of the interacting quantum ring has a large spin split and has the same appearance as that of a non-interacting ring (see section 3.3.4). This translates directly to the persistent current. It has the same form as the noninteracting current (Figure 2.5) apart from a difference in magnitude, being generally slightly larger. Figure 2.6 shows the ground state magnetic moment of the interacting system (within the Hartree-Fock approximation) for a screening constant of $\mu_s = 0.1$. The 2- and 3-electron spectrum is spin split due to the strength of interaction and as a result the magnetic moment is qualitatively similar to its noninteracting counterpart (compare the top panels of Figures 2.5 and 2.6). However, the situation for a larger number of electrons is markedly different. Where the energy spectrum shifts from spin-degenerate to spin-polarized, jumps appear in the magnetic moment. This has been observed by Maiti et al. [90] in an exact diagonalization of the 1D Hubbard model, although by a different mechanism. They fix the spin configuration of the system and investigate how the strength of the correlation affects the system. For an even higher number of electrons ($N_e > 10$) the spectrum is fully spin degenerate as the system is primarily controlled by kinetic energy term. The properties of the system can be described qualitatively by a model of noninteracting electrons with spin. The magnetic moment is therefore similar to that of the noninteracting system (Figure 2.5) except the current has for some values of the magnetic flux been inverted due to the double occupancy of levels.

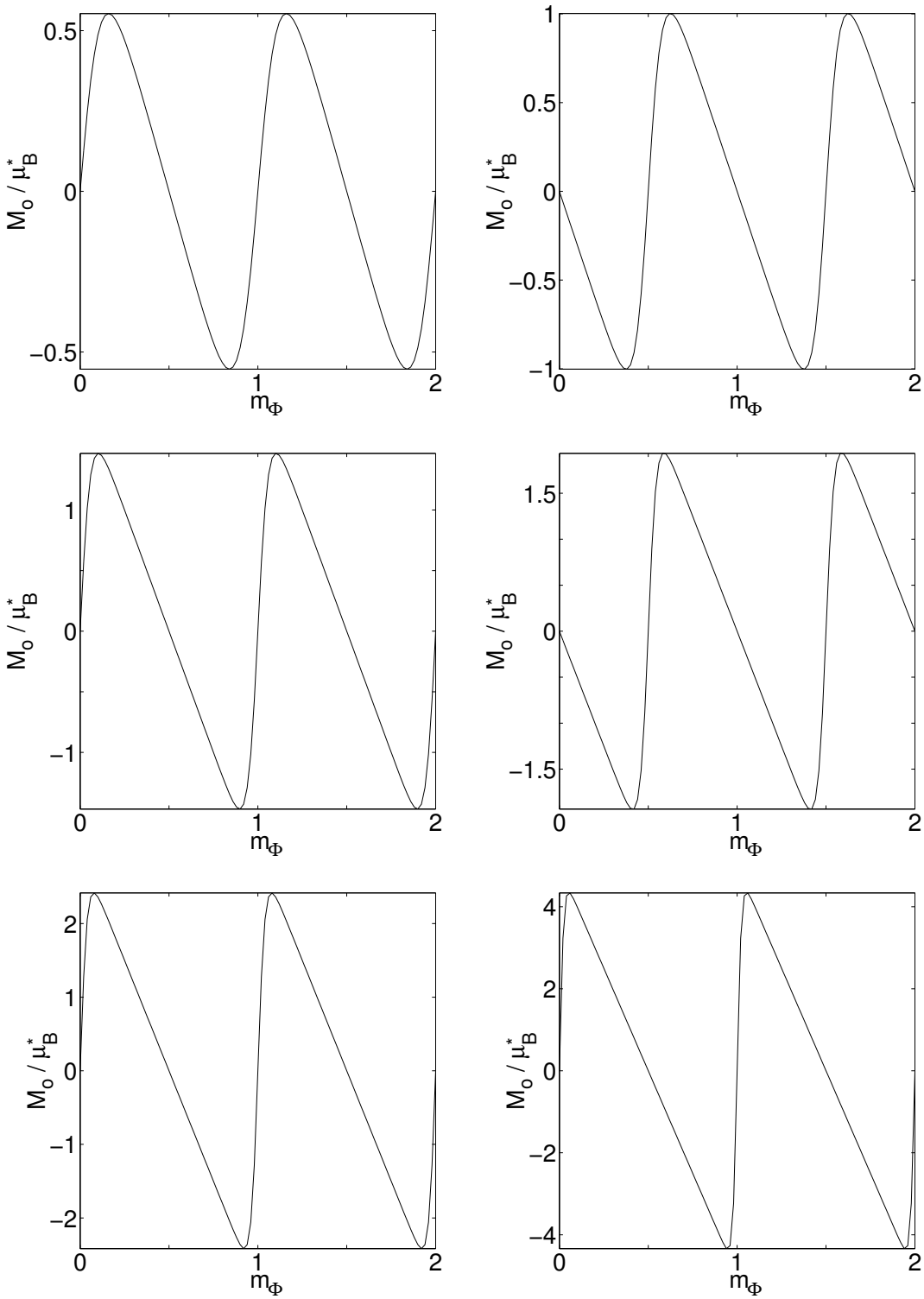

Figure 2.5: *Ground state orbital magnetic moment as a function of the external magnetic flux for 2 (top left), 3 (top right), 4 (middle left), 5 (middle right), 6 (bottom left) and 10 (bottom right) noninteracting electrons.*

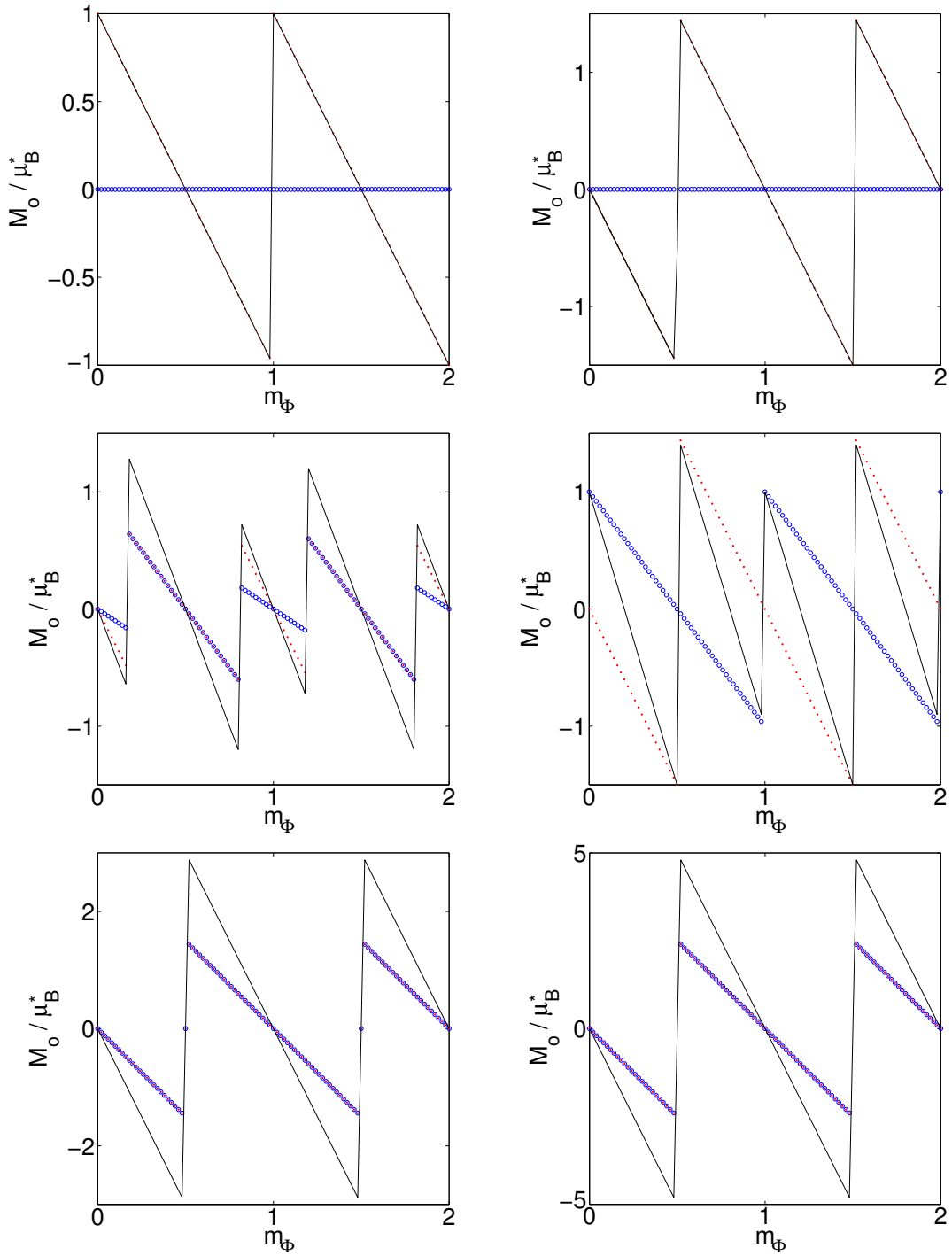

Figure 2.6: *Ground state orbital magnetic moment as a function of the external magnetic flux for 2 (top left), 3 (top right), 4 (middle left), 5 (middle right), 6 (bottom left) and 10 (bottom right) interacting electrons within the Hartree-Fock approximation. The screening parameter is* $\mu_s = 0.025$. *The points and circles denote the magnetic moment of spin up and spin down electrons respectively, the solid line is the total orbital magnetic moment.*

Chapter 3

Time Dependent Perturbation

In its ground state in a magnetic field, the one-dimensional quantum ring exhibits a circulating current, the persistent current. The current appears because the magnetic field breaks the left/right symmetry of the ring. The positive angular momentum states become less likely to be occupied and as a result the ring has a finite, negative angular momentum. In this Chapter the effect of a time-dependent perturbation on the persistent current is investigated and an attempt is made to answer the question as to why it changes.

When the electron gas on the ring is subject to a strong time-dependent perturbation its evolution is nonadiabatic and the concepts of single-electron energy levels and their occupation become poorly defined. Under these conditions it is convenient to study the time evolution of the density matrix. In this chapter the time-evolution equation of the density matrix is described and the method to solve it numerically is outlined. Following that the external perturbation is defined after which results are presented, the response of the orbital magnetic moment, the evolution of the electron density as well as the change in occupation of the angular momentum states.

3.1 Time Evolution of the Density Matrix

At time $t = 0$ the Hamiltonian of the system becomes time-dependent when an external perturbation of finite duration is turned on,

$$\hat{H}(t) = \hat{H}(0) + \hat{V}(t). \tag{3.1}$$

The density operator obeys the equation of motion

$$i\hbar \frac{d\hat{\rho}}{dt} = \left[\hat{H}(t), \hat{\rho}(t)\right], \tag{3.2}$$

however, the form of this equation is inconvenient for numerical evaluation. The time-evolution operator, defined by

$$\hat{\rho}(t) = \hat{T}(t)\ \hat{\rho}_0\ \hat{T}^\dagger(t), \quad \hat{\rho}_0 = \hat{\rho}(t=0), \tag{3.3}$$

has a simpler equation of motion [91]

$$\begin{aligned} i\hbar\dot{\hat{T}}(t) &= \hat{H}(t)\hat{T}(t) \\ -i\hbar\dot{\hat{T}}^\dagger(t) &= \hat{T}^\dagger(t)\hat{H}(t) \end{aligned} \tag{3.4}$$

which can be discretized in time and the Crank-Nicholson scheme used for the time-integration. A forward step in (3.4) gives

$$\begin{aligned} \hat{T}(t_{n+1}) - \hat{T}(t_n) &\simeq \frac{\Delta t}{i\hbar}\hat{H}(t_n)\hat{T}(t_n) \\ \Rightarrow \quad \hat{T}(t_{n+1}) &\simeq \left[\mathbb{1} + \frac{\Delta t}{i\hbar}\hat{H}(t_n)\right]\hat{T}(t_n) \end{aligned} \tag{3.5}$$

and a backwards step gives

$$\begin{aligned} \hat{T}(t_n) - \hat{T}(t_{n-1}) &\simeq \frac{\Delta t}{i\hbar}\hat{H}(t_n)\hat{T}(t_n) \\ \xrightarrow{n\to n+1} \quad \hat{T}(t_{n+1}) - \hat{T}(t_n) &\simeq \frac{\Delta t}{i\hbar}\hat{H}(t_{n+1})\hat{T}(t_{n+1}) \\ \Rightarrow \quad \left[\mathbb{1} - \frac{\Delta t}{i\hbar}\hat{H}(t_{n+1})\right]\hat{T}(t_{n+1}) &\simeq \hat{T}(t_n). \end{aligned} \tag{3.6}$$

Taking the average of (3.5) and (3.6) results in

$$\left[\mathbb{1} - \frac{\Delta t}{2i\hbar}\hat{H}(t_{n+1})\right]\hat{T}(t_{n+1}) \simeq \left[\mathbb{1} + \frac{\Delta t}{2i\hbar}\hat{H}(t_n)\right]\hat{T}(t_n), \tag{3.7}$$

or

$$\left[\mathbb{1} + \frac{i\Delta t}{2\hbar}\hat{H}(t_n)\right]\hat{T}(t_n) \simeq \left[\mathbb{1} - \frac{i\Delta t}{2\hbar}\hat{H}(t_{n-1})\right]\hat{T}(t_{n-1}). \tag{3.8}$$

In the basis of $\hat{h}_0$ (2.10) the time evolution equation (3.8) becomes a matrix equation of the form $AT = B$ with the boundary condition $T(0) = \mathbb{1}$. Eq. (3.8) together with (3.3) specifies the state of the system at any time instant and relevant physical properties can be calculated in terms of the density matrix by (2.20). Specifically, the magnetic moment at each timestep is given by (2.72) with $H_{lm} = H_{lm}(t)$ and $\rho_{ml} = \rho_{ml}(t)$.

When the Coulomb interaction is included, (3.8) must be solved iteratively. The ground state is obtained as described in section 3.3.3. When the perturbation is acting on the system, the Hamiltonian of the previous timestep $\hat{H}(t_{n-1})$ is known, but $\hat{H}(t_n)$ depends on the time evolution operator $\hat{T}(t_n)$ through the density matrix. To obtain $\hat{H}(t_n)$ it is first approximated by using the density matrix from the last timestep and then (3.8) is solved iteratively until self-consistency is reached, i.e. until the change in $\hat{H}(t_n)$ becomes negligible.

3.2 The External Perturbation

The external time-dependent perturbation chosen is a short-lived radiation pulse with a spatial distribution resembling dipole radiation

$$V(t) = V_0 \cos\theta \, e^{-\Gamma t} \sin(\omega_1 t) \sin(\omega t) \Theta(\pi - \omega_1 t) \tag{3.9}$$

where Θ is the Heaviside step function. The exponential factor limits the life-time of the pulse and the sine functions, with an envelope frequency ω_1 and a base frequency ω, ensure that the perturbation has an initial value of zero. It is important to note that the spatial distribution of the pulse does not break the left/right symmetry of the system. Both the angular and time-dependence of the perturbation are shown in Fig. 3.1.

3.3 Dynamic Magnetic Moment

First the results for the noninteracting ring will be presented followed by those of the interacting quantum ring. The absence of a confinement potential (i.e. the one-dimensionality) in the noninteracting one-dimensional ring causes the magnetic moment to reach a steady state value immediately after the perturbation has been turned off, as shown in Figure 3.2. This is quite different from the response of a ring of finite-width [67] where the magnetic moment oscillates after the excitation pulse vanishes, a consequence of the coupling between radial and angular density oscillations. As shown in Figure 3.3 for a one-dimensional ring containing one electron, the magnetic moment after the perturbation has vanished is different from the ground state magnetic moment, at a finite magnetic field. It should be stressed that in the model discussed here no means of energy dissipation is included. Therefore, by applying the perturbation, the system is brought to an excited state in which it will remain forever. For low

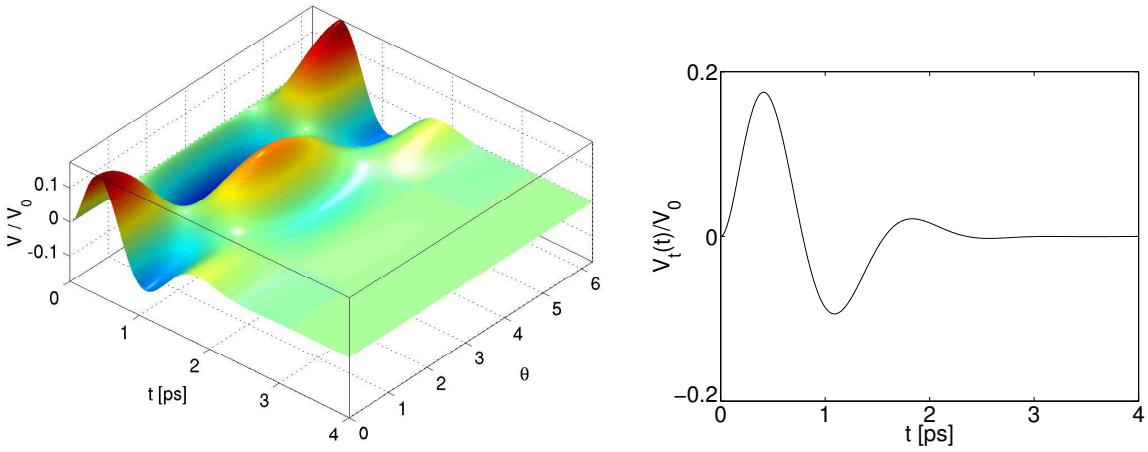

Figure 3.1: **Left:** *The external perturbation along the ring as a function of time.* **Right:** *Time-dependent part of the pulse for* $\theta = 0$*. The parameter values are* $\hbar\omega_1 = 0.658$ *meV,* $\hbar\omega = 2.63$ *meV and* $\Gamma = 2/ps$*.*

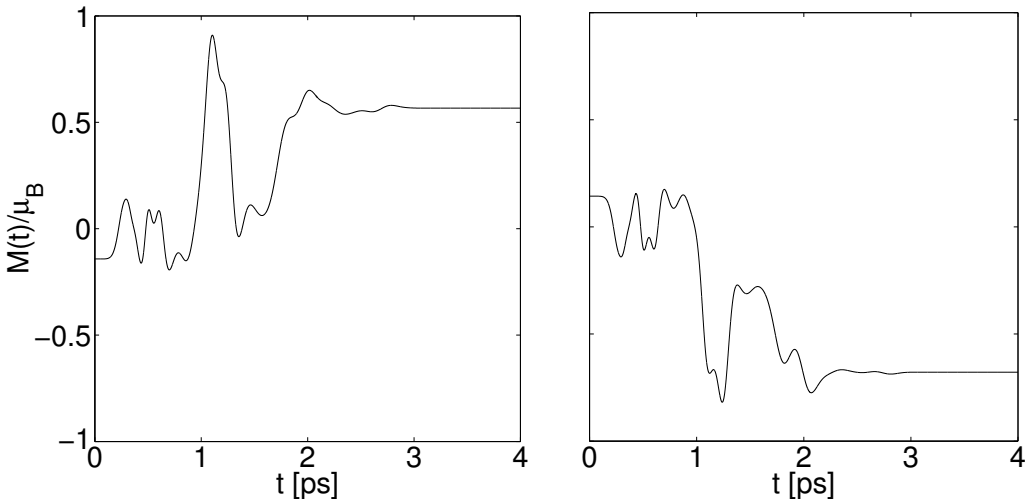

Figure 3.2: *Orbital magnetic moment* $M_o(t)$ *as a function of time for 1 electron on the ring.* **Left:** $m_\Phi = 0.25$ $(B = 1.71T)$*.* **Right:** $m_\Phi = 0.7$ $(B = 4.7T)$*. The strength of the perturbation is* $V_0 = 100E_0$ *(0.29 eV), with the other parameters given in the caption of Figure 3.1.*

values of the magnetic field, the magnetic moment (and thus the current) increases proportional to the perturbation strength. When $B \sim 1$ T a drastic nonlinear change occurs. The magnetic moment changes sign, implying that the direction of the current has changed, and for the remaining magnetic field values shown, the current after excitation is in anti-phase with the equilibrium persistent current and larger in magnitude. At $m_\Phi = 0.5$ ($B = 3.36$ T) the magnetic moment goes to zero even after the system has been excited. The reason for this becomes clear when looking at the energy spectrum of the ring, shown in Figure 2.1 page 8. At integer and half-integer values of the magnetic flux the slopes of degenerate (crossing) levels have opposite signs. Being proportional to the slope, the currents of crossing levels are cancelled out and in effect there can be no current in the system. It has therefore no effect to excite the ring to a higher energy state. At these values of m_Φ the magnetic field is not able to break the left/right symmetry of the system and since the external perturbation is left/right symmetric it cannot induce a net current.

The current generated by the perturbation depends strongly on the number of electrons on the ring. As an example Figure 3.4 shows the initial and final magnetic moment for eight electrons on the ring. The perturbation causes a decrease in the magnitude of the persistent current and is not able to change its direction for the range of magnetic field strengths shown here. With increasing number of electrons more energy is needed to excite the system to a state with a very different current from the ground state persistent current.

When the temperature is increased the ground state persistent current gradually disappears. At a higher temperature the occupation of single-electron states is more or less evenly distributed over a larger range of angular momentum values. Consequently the occupation of each level is quite small and due to the cancellation between successive bands the current disappears. Even though the temperature kills the ground state persistent current the perturbation is able to excite a current along the ring even at $T = 100$°C as shown in Figure (3.5).

When the interaction between electrons is included in the Hartree-Fock approximation the response of the system to a time-dependent perturbation is sensitive to spin effects. When there are equal amounts of up and down spin electrons the evolution of the orbital magnetic moment is similar to that of a noninteracting quantum ring, as shown in Figure 3.6 for eight interacting electrons. The magnetic moments $M_o^\uparrow$ and $M_o^\downarrow$ are equal in the groundstate and because the energy spectrum is spin-degenerate, i.e. the spatial wave functions of opposite spin direction are the same, the two spin

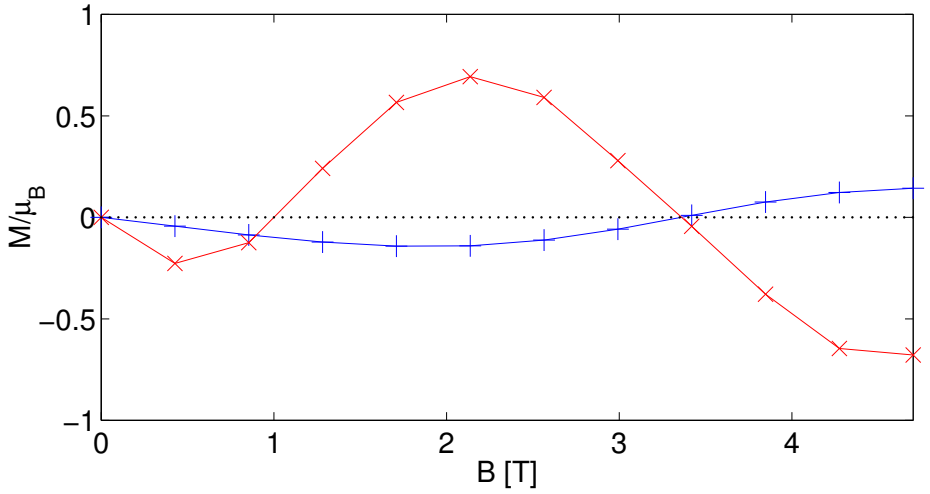

Figure 3.3: *Equilibrium magnetic moment $M_o(0)$ (+) and the magnetic moment $M_o(t_f)$ (×) after the radiation pulse has vanished for one electron. Here t_f denotes the final timestep. The strength of the perturbation is $V_0 = 100E_0$ (0.29 eV), with the other parameters given in the caption of Figure 3.1.*

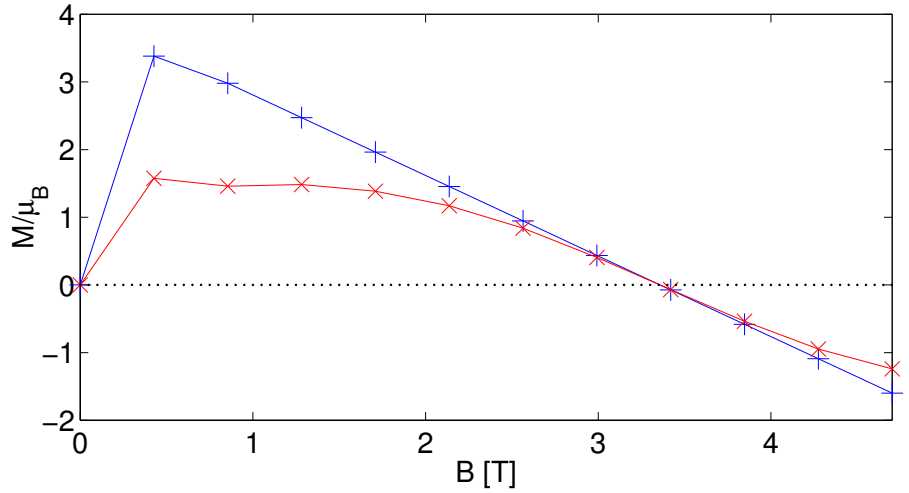

Figure 3.4: *Equilibrium magnetic moment $M_o(0)$ (+) and the magnetic moment $M_o(t_f)$ (×) after the radiation pulse has vanished for 8 electrons. Here t_f denotes the final timestep. The strength of the perturbation is $V_0 = 100E_0$ (0.29 eV), with the other parameters given in the caption of Figure 3.1.*

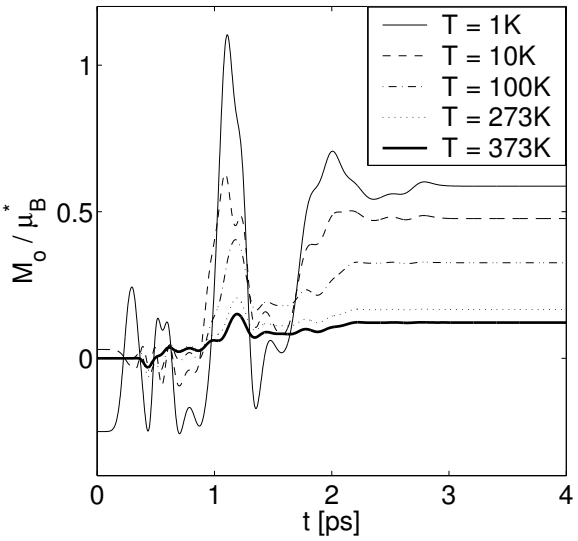

Figure 3.5: *The temperature dependence of the orbital magnetic moment* $M_o(t)$ *for a single electron on the ring in a magnetic flux of* $m_\Phi = 0.25$. *The strength of the perturbation is* $V_0 = 100E_0$ *(0.29 eV), with the other parameters given in the caption of Figure 3.1.*

densities evolve in the same manner. As in the case of noninteracting electrons the magnetic moment reaches a constant value when the perturbation vanishes, which is different from the ground state value.

When the ground state of the interacting system is spin split and there is an unequal amount of up and down spin electrons, the magnetic moments of opposite spin evolve differently. However, after the pulse has disappeared the total magnetic moment must remain constant as there is no force in the system to sustain oscillations. There is no confinement or modulation and no dissipation of energy. Since the magnetic moments of opposite spin direction are unequal at the time when the pulse vanishes, they start oscillating in anti-phase.

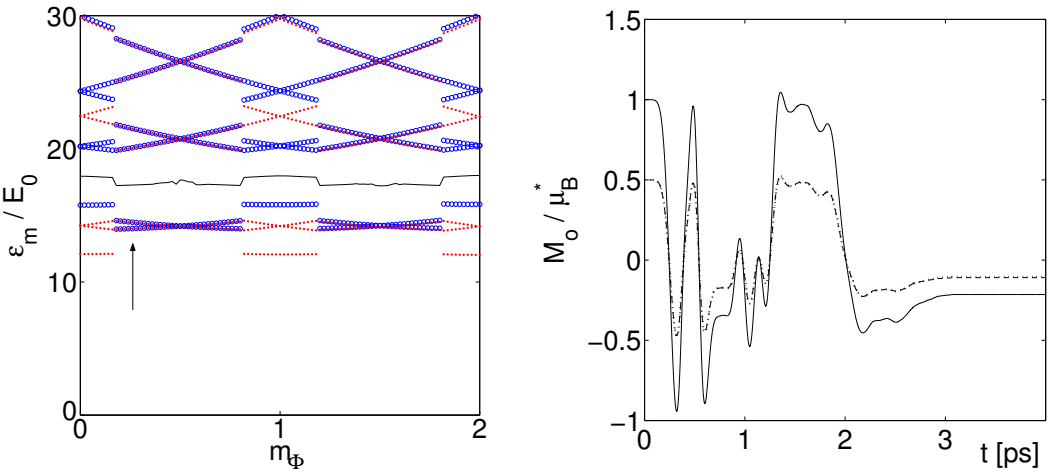

Figure 3.6: **Left:** *Energy spectrum of a ring containing 4 interacting electrons. The energy is given in units of* $E_0 = \hbar^2/2m^*r_0^2$ *and the screening parameter is* $\mu_s = 0.025$*. Points and circles denote the energy of spin up and spin down electrons respectively, the solid line is the chemical potential.* **Right:** *Orbital magnetic moment* $M_o(t)$ *as a function of time for* $m_\Phi = 0.25$*, indicated by an arrow in the left panel. The dotted line is the magnetic moment of spin down electrons, the dash-dotted line the magnetic moment of spin up electrons (hidden behind dotted line) and the solid line is the total magnetic moment.*

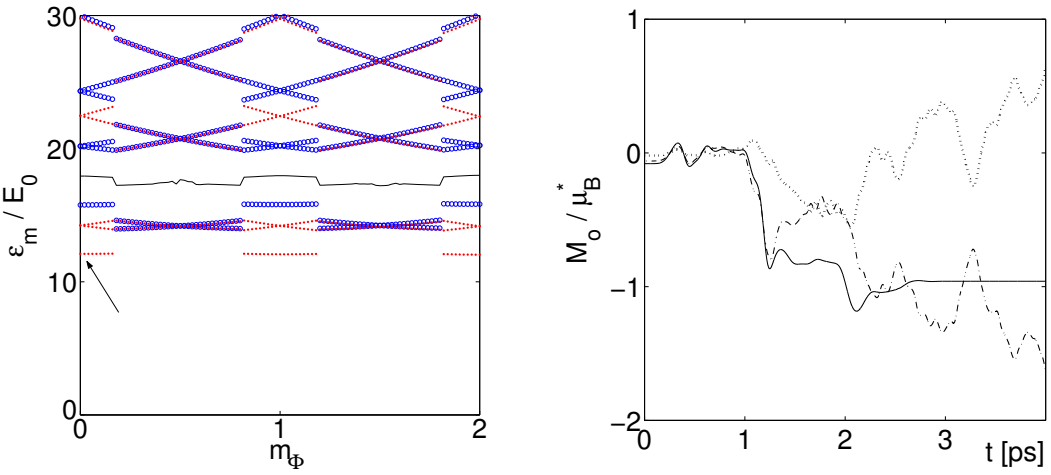

Figure 3.7: **Left:** *Energy spectrum of a ring containing 4 interacting electrons. The energy is given in units of* $E_0 = \hbar^2/2m^*r_0^2$ *and the screening parameter is* $\mu_s = 0.025$*. Points and circles denote the energy of spin up and spin down electrons respectively, the solid line is the chemical potential.* **Right:** *Orbital magnetic moment* $M_o(t)$ *as a function of time for* $M_\Phi = 0.02$*, indicated by an arrow in the left panel. The dotted line is the magnetic moment of spin down electrons, the dash-dotted line the magnetic moment of spin up electrons and the solid line is the total magnetic moment.*

3.4 Collective Oscillations

The time evolution of the electron density in the ring is shown in Fig. 3.8 for a ring with eight noninteracting electrons in a magnetic flux of $m_\Phi = 0.21$ ($B = 1.41$ T). The perturbation clearly induces angular density oscillations that continue after the pulse has vanished and travel anti-clockwise around the ring. In a zero magnetic field the oscillations do not travel around the ring, a further indication that the perturbation does not break the left/right symmetry of the system. The density profile follows closely the shape of the excitation pulse (shown in Figure 3.1, page 32). However, when the peak of the pulse is reached, collective oscillations are superimposed on the larger oscillations caused by the pulse, and are not suppressed when it vanishes. A closer inspection of the density matrix reveals the origin of these oscillations. When the perturbation dies out the Hamiltonian of the system becomes time-independent. The state of the system is a linear combination of the eigenstates of the Hamiltonian h_0. The coefficients of the expansion thus acquire a time-dependent phase factor whose value depends on the energy of the eigenstate. Therefore, after the pulse has vanished, the diagonal elements (the populations) of the density matrix, which describe the probability for a state to be occupied, remain constant. However, the off-diagonal elements (the coherences), which describe the interference between the different basis states, change with time. These changes lead directly to oscillations in the electron density. A similar effect can be seen in a two-level (1D) quantum well. If an electron in a quantum well is initially in a linear combination of two eigenstates of the Hamiltonian and allowed to evolve with time, then the density oscillates back and forth between the walls of the well. In the previous section we saw that the magnetic moment remains constant after the perturbation vanishes. This is a direct consequence of the time-independence of the diagonal elements of the density matrix.

When the interaction between electrons is included the oscillation peaks are more pronounced due to the Coulomb interaction which forces the electrons apart. The oscillations travel in the opposite direction, as shown in Figure 3.9. Since the ground state of the interacting system has the angular momentum states $m^\uparrow = m^\downarrow = 0, \pm 1, 2$ occupied, whereas in the model excluding interactions $m = 0, \pm 1, \pm 2, \pm 3, 4$ are occupied, it is to be expected that the time evolution under the influence of a perturbation is different.

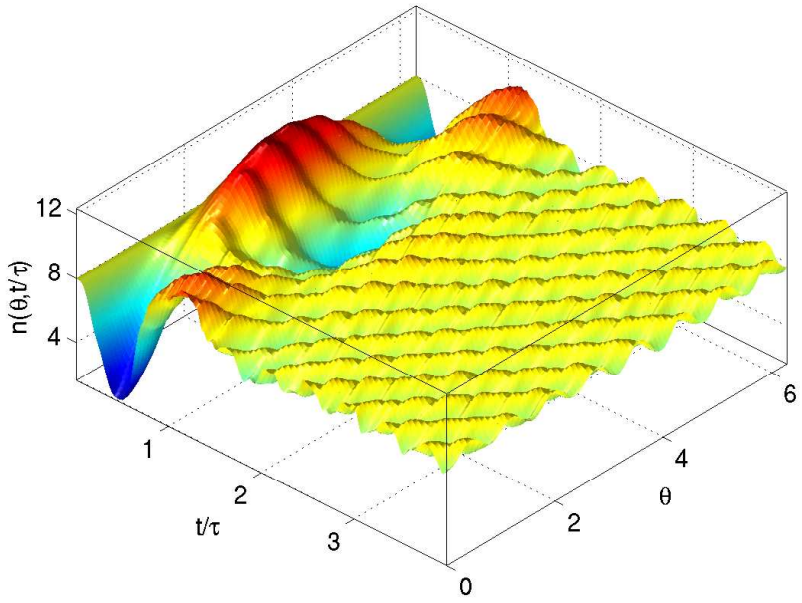

Figure 3.8: *Electron density as a function of angle and time for 8 noninteracting electrons on the ring in a magnetic flux of* $m_\Phi = 0.21$ *(*$B = 1.41T$*). The strength of the perturbation is* $V_0 = 100E_0$ *(0.29 eV), with the other parameters given in the caption of Figure 3.1.*

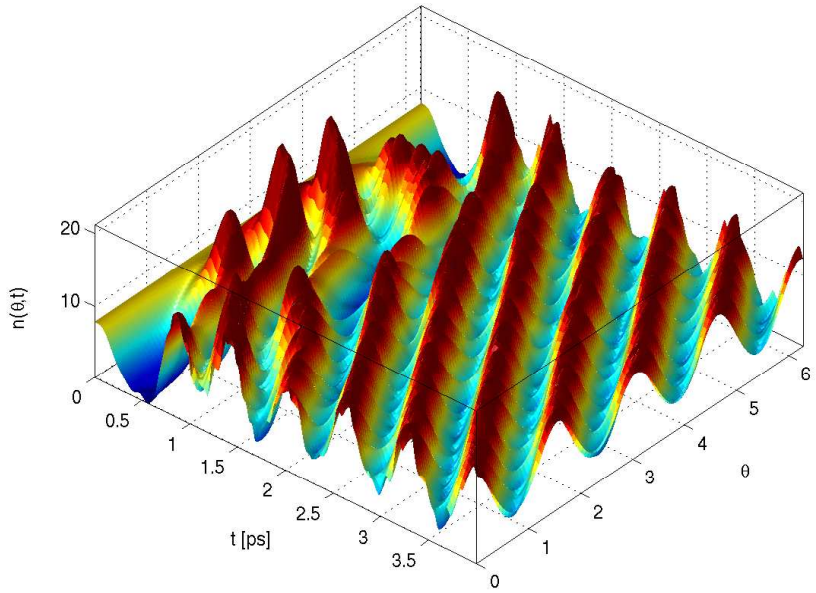

Figure 3.9: *Electron density as a function of angle and time for 8 interacting electrons on the ring (*$\mu_s = 0.025$*) in a magnetic flux of* $m_\Phi = 0.21$ *(*$B = 1.41T$*). The strength of the perturbation is* $V_0 = 100E_0$ *(0.29 eV), with the other parameters given in the caption of Figure 3.1.*

3.5 Occupation Changes

By inspecting the diagonal elements of the density matrix it becomes clear that the persistent current is changed through a modified occupation of the single-electron states. After the perturbation has been turned off, the combination of angular momentum states is different from that of the ground state and thus the persistent current is changed. Figure 3.10 shows the occupation of the lowest lying angular momentum states for a one-electron ring in a magnetic flux of $m_\Phi = 0.25$ ($B = 1.68$ T) before

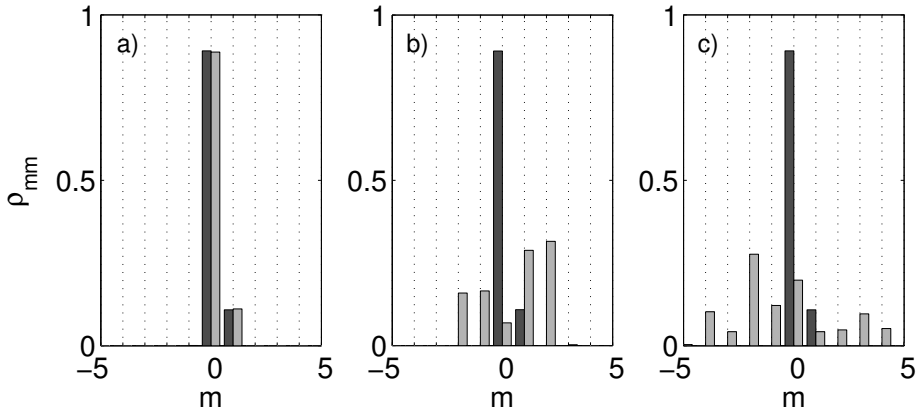

Figure 3.10: *Diagonal elements of the density matrix for a ring with one electron in a magnetic flux of $m_\Phi = 0.25$ ($B = 1.68$ T) and different perturbation strength, m denotes the quantum number characterizing the basis states of h_0. The ground state occupation is shown with darkgrey bars, and to the right of them the lightgrey bars give the occupation after excitation. a) $V_0 = 1$ meV ($0.34E_0$), b) $V_0 = 0.1$ eV ($34.5E_0$) and c) $V_0 = 1$ eV ($344.8E_0$).*

and after excitation for different strengths of the perturbation. For a weak perturbation, changes in the occupation are very small and should be captured by the linear response method. As the pulse strength increases more angular momentum m states are involved, even those high above the Fermi level. If the number of electrons on the ring is increased, higher strength is required for a nonlinear change in the occupation.

Chapter 4

The Effect of Asymmetry

The appearance of a persistent current in quantum rings relies on the breaking of their left/right symmetry. In an external magnetic field the ground state of the system moves to higher angular momentum states to minimize the effective kinetic energy. The occupation of states with opposite but equal current is thus distorted and a net current flows along the ring. In this chapter other means of symmetry breaking and their effect on the persistent current of the ring are investigated. The electron spin as well as their mutual interaction will be neglected. To model the ring containing $N_e = 3$ electrons in a GaAs heterostructure the effective mass of the electron is $m^* = 0.067\,m$ and the effective g-factor $g^* = -0.44$. The radius of the ring is chosen to be $r_0 = 14$ nm and the temperature $T = 4$K.

As Figures 3.3 and 3.4 show, the symmetric external perturbation (3.9) cannot induce a current along the ring without the breaking of left/right symmetry by the magnetic field. The question whether a spatially asymmetric perturbation can induce a current in the ring at a zero magnetic field naturally arises. The perturbation has the same time-dependence as (3.9)

$$V_A(t) = W(\theta)\, e^{-\Gamma t} \sin(\omega_1 t) \sin(\omega_2 t), \tag{4.1}$$

but has an asymmetric spatial distribution given by a combination of a dipole and a rotated quadrupole fields

$$W(\theta) = A\big(\cos\theta + \cos 2(\theta + \theta_0)\big), \tag{4.2}$$

where θ_0 is the rotation angle. The perturbation is depicted in Figure 4.1 for $\theta_0 = 0°$, when the pulse is symmetric, and for $\theta_0 = 45°$, when it is asymmetric. Initially, the system is in its ground state where right and left rotating states, $|m\rangle$ and $|-m\rangle$, are equally occupied and the current is consequently zero. As expected, the left panel of Figure 4.2 shows that if the external pulse, like the ring itself, is left/right symmetric

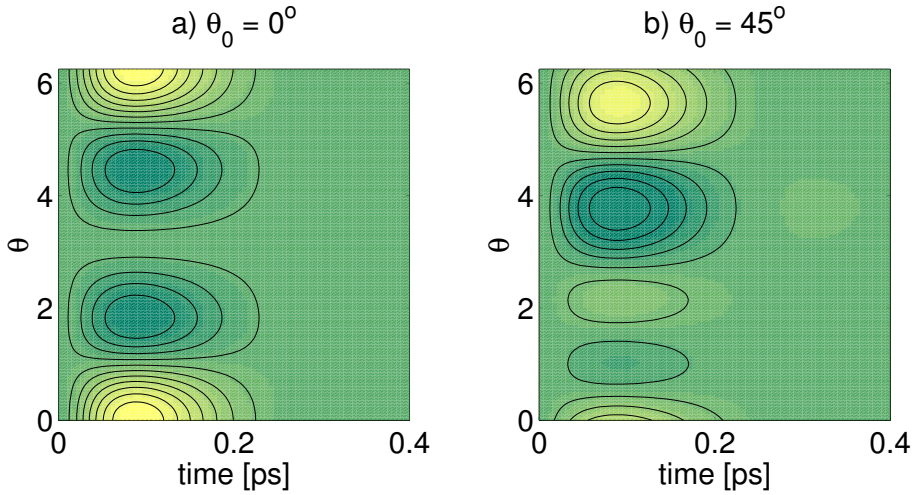

Figure 4.1: *Spatial distribution of the external potential pulse as a function of time for (a) $\theta_0 = 0°$ and (b) $\theta_0 = 45°$. The parameter values are $\hbar\omega_1 = 2.83$ meV, $\hbar\omega_2 = 8.11$ meV, $\hbar\Gamma = 11.32$ meV and $A = 67.68$ meV. The frequencies are chosen to be comparable to the Bohr frequencies $\hbar\omega_{01} = 2.89$ meV and $\hbar\omega_{12} = 8.6$ meV. Bright/yellow regions indicate maxima in the potential.*

($\theta_0 = 0$) a current can not be induced since the occupation of angular momentum states remains symmetric. However, by introducing an assymmetry to the perturbation a net (constant) current appears. For this set of parameters the excited current reaches a maximum value for a rotation angle of $\theta_0 = 45°$ and decreases towards zero for $\theta_0 \to 90°$. For a weak excitation pulse a perturbation analysis to 2^{nd} order reveals that the difference in transition probability between states $|1\rangle$ and $|-1\rangle$, for a single electron initially in the ground state $|0\rangle$, is proportional to $\sin 2\theta_0$

$$\mathcal{P}_{0,1}(t) - \mathcal{P}_{0,-1}(t) = F(t) \sin 2\theta_0 \tag{4.3}$$

where $F(t)$ is a double integral which depends on the parameters of the external perturbation. This implies that for a rotation angle of $\theta_0 = 45°$ the resulting current is at maximum, as was the case in Figure 4.2 (left panel). However, a single-particle perturbation analysis is not fully applicable to the system considered here, in part because the number of electrons on the ring is greater than one and the perturbation is stronger than the stationary Hamiltonian h_0. The exact values of the perturbation parameters have a strong influence on the resulting current, as is evident from the right panel of Figure 4.2 which depicts the induced magnetic moment as a function of the rotation angle for three values of Γ. As Γ decreases the maximum of the magnetic moment shifts away from $\theta_0 = 45°$ indicating that the results have a more complex dependence on the exact form of the perturbation, in particular the strength.

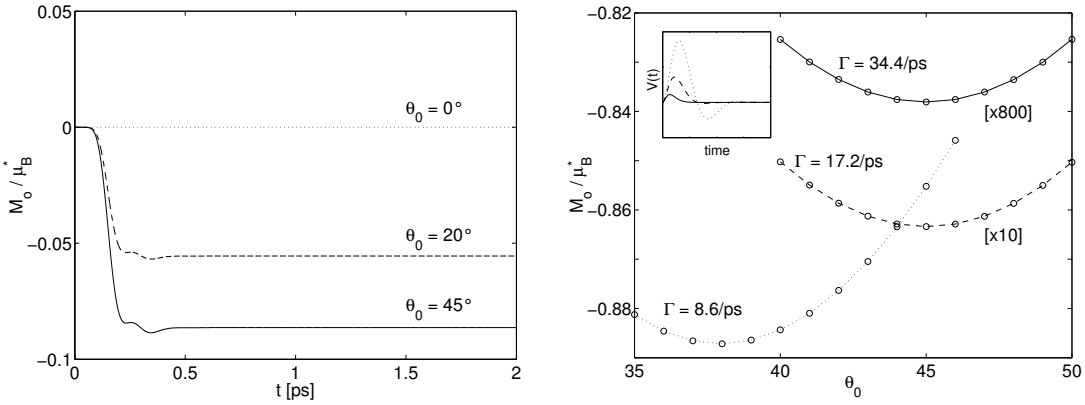

Figure 4.2: **Left**: *The time evolution of the orbital magnetic moment for three values of the rotation angle* $\theta_0 = 0°, 20°, 45°$. **Right**: *The induced values of the orbital magnetic moment as a function of the rotation angle* θ_0 *for three values of* Γ. *The scale of the upper two curves has been magnified as indicated. The inset depicts the time dependent part of the perturbation for the three situations. The parameter values for the external perturbation are given in the caption of Fig. 4.1.*

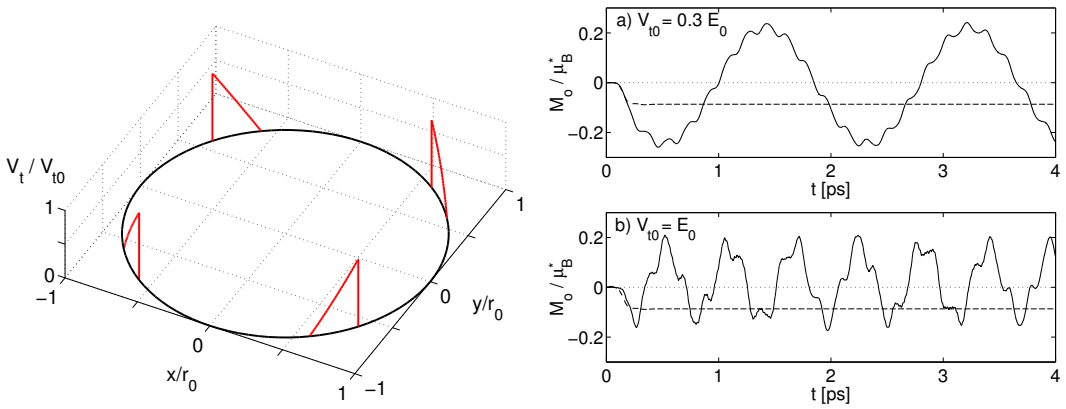

Figure 4.3: **Left**: *Ratchet potential.* **Right**: *The orbital magnetic moment as a function of time when the system is perturbed by the asymmetric pulse (4.1) with* $\theta_0 = 45°$. *The parameter values for the perturbation are given in the caption of Fig. 4.1. The strength of the ratchet potential is a)* $V_{t0} = 0.3E_0$ *and b)* $V_{t0} = E_0$, *with* $E_0 = \hbar^2/2m^*r_0^2$. *The dashed curve is the time-evolution of the magnetic moment for a pure ring.*

The magnitude of the current generated in the system by a left/right asymmetric excitation can be reduced by the inclusion of a ratchet potential as shown in Figure 4.3. The background potential causes oscillations in the induced magnetic moment whose frequency grows with the height of the ratchets. Even for a very weak potential the oscillations persist and the average current vanishes. It is interesting to note that the period of oscillation can be much larger than that of the applied perturbation.

Another way of breaking the left/right symmetry of the ring is by the inclusion of an asymmetric background potential and perturbing the system with the symmetric pulse (3.9). Two types of potentials have been tested, a sawtooth (ratchet) potential defined by

$$V_r(\theta) = \begin{cases} \frac{2V_{r0}}{\pi}\,\theta, & \theta \in \left[0, \frac{\pi}{2}\right] \\ \frac{2V_{r0}}{\pi}\,\left(\theta - \frac{\pi}{2}\right), & \theta \in \left(\frac{\pi}{2}, \pi\right] \\ \frac{V_{r0}}{\pi}\,\left(\theta - \pi\right), & \theta \in \left(\pi, 2\pi\right), \end{cases} \tag{4.4}$$

shown in the left panel of Figure 4.1, and a dipole-rotated quadrupole field

$$V_d(\theta) = V_{d0}\left(\cos\theta + \cos 2(\theta + \theta_d)\right), \tag{4.5}$$

shown in the right panel of Figure 4.4. The results, shown in Figures 4.5 and 4.6, indicate

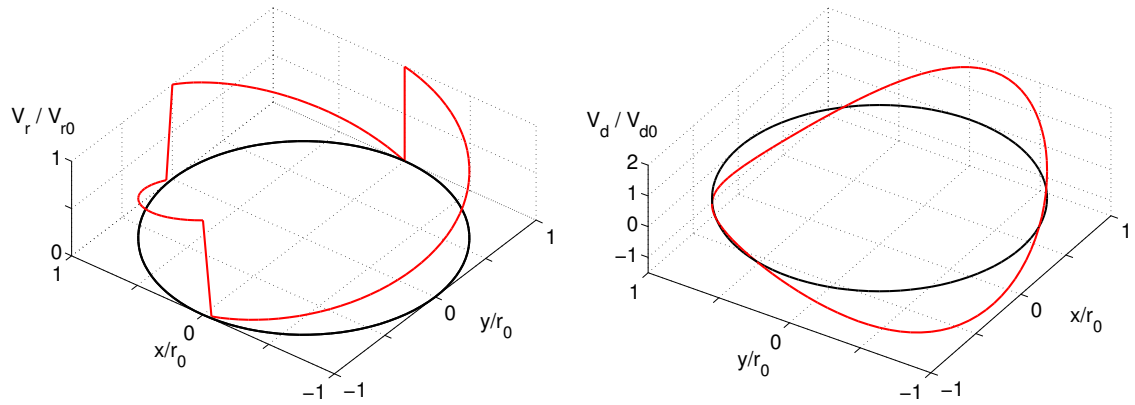

Figure 4.4: **Left**: *Asymmetric ratchet potential (4.4).* **Right**: *Dipole-rotated quadrupole potential (4.5 with* $\theta_d = 45°$*).*

that an asymmetric modulation of the quantum ring is not effective in aiding the generation of a net current by a symmetric external perturbation. The background potentials cause oscillations in the induced magnetic moment whose mean value is very near to zero, i.e. no steady current has been generated. High frequency dipole oscillations due to the external pulse are superimposed on larger oscillations whose

frequency increases with the strength of the modulation. Even for a very weak modulation the oscillations still appear, with a period much larger than that of the applied perturbation, as the right panel of Figure 4.6 shows.

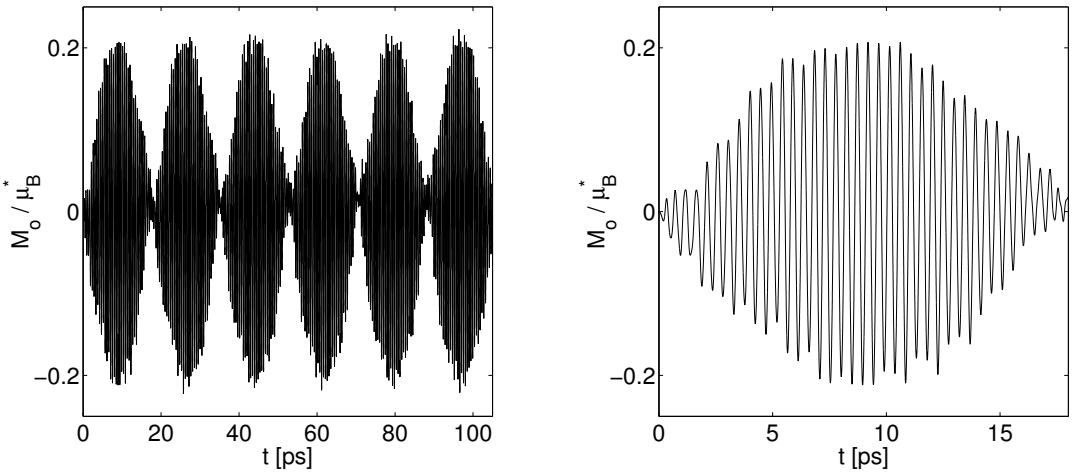

Figure 4.5: *The time-evolution of the orbital magnetic moment of a ring modulated by the ratchet potential (4.4) when subject to the symmetric pulse (3.9). The perturbation parameters are listed in the caption of Figure 4.1. The strength of the ratchet modulation is* $V_{r0} = E_0$*, with* $E_0 = \hbar^2/2m^*r_0^2$*. The left panel shows a closer look at one "beat" in the right panel.*

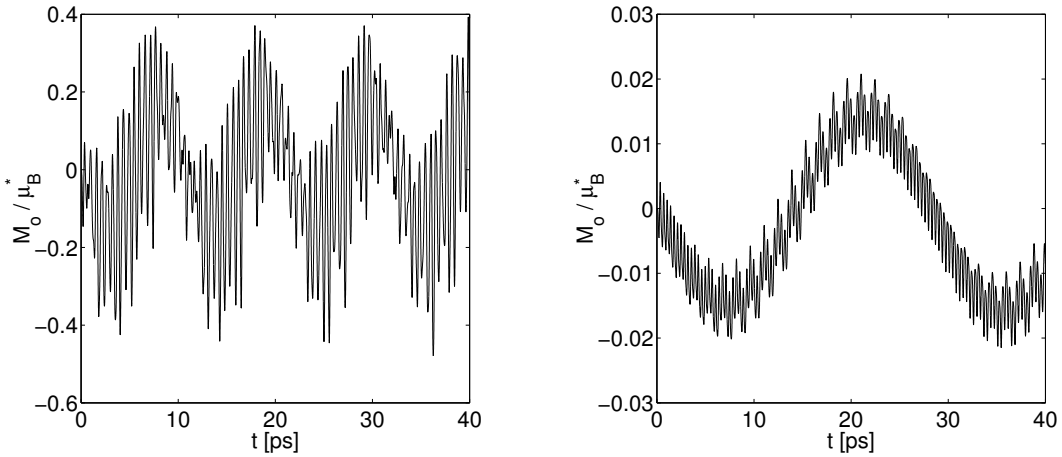

Figure 4.6: *The time-evolution of the orbital magnetic moment of a ring modulated by the dipole-rotated quadrupole potential (4.5, with* $\theta_d = 45°$*) when subject to the symmetric pulse (3.9). The perturbation parameters are listed in the caption of Figure 4.1. The strength of the ratchet modulation is* $V_{d0} = E_0 = 8.42k_BT$ *(left) and* $V_{d0} = 0.05E_0 = 0.42k_BT$ *(right).*

Chapter 5

Conclusions

The one property of the quantum ring which has recieved the greatest interest is its persistent current which appears when the ring is placed in an external magnetic field. The persistent current appears due to breaking the left/right symmetry. In a magnetic field the ground state of the system moves to higher negative angular momentum in order to minimize its effective kinetic energy. Occupation of states with a positive angular momentum becomes depleted and a constant current flows along the ring. Due to the periodicity of the energy spectrum, the persistent current is periodic in the magnetic flux threading the ring.

When the interaction between electrons is included within the Hartree-Fock approximation the properties of the system can be divided into three cases depending on the strength of the Coulomb interaction. When the ring contains a large number of electrons the kinetic energy is the main force of influence on the system and consequently the energy spectrum and therefore the persistent current are qualitatively similar to that predicted by a noninteracting model with spin included. If there are few electrons on the ring the Coulomb interaction has a much stronger influence than the kinetic energy. Due to the exchange interaction the system becomes spin polarized, i.e. only electrons of the same spin are present in the system. In this case the energy spectrum and thus the current is similar to that of a ring containing noninteracting spinless electrons. In between these limits the inclusion of the Coulomb interaction produces features which cannot be seen in a model of noninteracting electrons. In the case of an even number of electrons the groundstate shifts between a spin degenerate ($S = 0$) and a spin polarized ($S = 1$) configuration. For an odd number of electrons there is always some degree of spin splitting due to the inequal number of electrons of opposite spin. The persistent current displays kink-like structures which, for an even number of electrons, gradually disappear with increasing number of electrons. For odd

electrons the kinks remain quite pronounced at least up to $N_e = 9$.

The persistent current can be manipulated by applying an external time-dependent perturbation which resembles a dipole radiation field. The perturbation excites the system to a higher energy state with a different combination of angular momentum states than that of the ground state, thus changing the persistent current. In a pure one-dimensional ring there are no forces to sustain oscillations in the current after excitation, it reaches an equilibrium value immediately when the perturbation vanishes. At the points where the magnetic field is not able to break the left/right symmetry of the ring and the ground state persistent current disappears, the (symmetric) perturbation cannot induce a current in the ring. However, by introducing an asymmetry to the perturbation a constant current can be generated at a zero magnetic field. The appearance of a persistent current in quantum rings relies on the breaking of their left/right symmetry. However, if the ring is modulated by an asymmetric background potential the symmetric pulse causes an oscillating current whose period can be very large compared to that of the pulse.

Appendix A

Fock Matrix Elements

When the plane wave basis of $\hat{h}_0$ (2.10) is used to represent the single-electron states of the Slater determinant, the matrix elements of the Coulomb interaction terms can be calculated analytically. The matrix elements of the Fock operator (2.49) include two-electron integrals of the type

$$\begin{aligned}\langle\phi_l\phi_n|\phi_m\phi_p\rangle &= \int d\mathbf{r}\, d\mathbf{r}'\, \phi_l^*(\mathbf{r})\phi_m(\mathbf{r})\, |\mathbf{r}-\mathbf{r}'|^{-1}\, \phi_n^*(\mathbf{r}')\phi_p(\mathbf{r}') \\ &= \int r_0^2\, d\theta\, d\theta'\, \frac{e^{il\theta}e^{-im\theta}}{2\pi r_0} \frac{1}{r_0\sqrt{\sin^2((\theta-\theta')/2)+\mu_s^2}} \frac{e^{in\theta'}e^{-ip\theta'}}{2\pi r_0} \\ &= \frac{1}{4\pi^2 r_0} \int d\theta\, e^{i(l-m)\theta} \int d\theta'\, \frac{e^{i(n-p)\theta'}}{\sqrt{\sin^2((\theta-\theta')/2)+\mu_s^2}}\end{aligned} \tag{A.1}$$

where we have inserted the interaction kernel

$$|\mathbf{r}-\mathbf{r}'|^{-1} \to \left(r_0\sqrt{\sin^2((\theta-\theta')/2)+\mu_s^2}\right)^{-1} \tag{A.2}$$

describing an interaction along a straight line connecting two electrons at θ and θ'. To eliminate the singularity of the Coulomb interaction at $\theta=\theta'$ a screening constant μ_s is inserted. With a change of integration variables $x=(\theta-\theta')/2$ (A.1) becomes

$$\langle\phi_l\phi_m|\phi_n\phi_p\rangle = \frac{1}{2\pi^2 r_0} \int d\theta\, e^{i(l-m)\theta}\, e^{i(n-p)\theta} \int_{\theta/2-\pi}^{\theta/2} dx\, \frac{e^{-i2(n-p)x}}{\sqrt{\sin^2 x+\mu_s^2}}. \tag{A.3}$$

To calculate the inner integral, which we will denote $K_{pn}(\theta)$, we rewrite the interaction kernel using the relation

$$\frac{1}{\sqrt{\rho^2+z^2}} = \int_0^\infty dk\, e^{-|z|k} J_0(k\rho), \tag{A.4}$$

where $J_0(x)$ is the Bessel function of the first kind of order zero. On inserting this K_{pn} becomes ($\mu_s > 0$)

$$\begin{aligned} K_{pn}(\theta) &= \int_{\theta/2-\pi}^{\theta/2} dx\, e^{i2(p-n)x} \int_0^\infty dk\, e^{-\mu_s k} J_0(k\sin x) \\ &= \int_0^\infty dk\, e^{-\mu_s k} \int_{\theta/2-\pi}^{\theta/2} dx\, e^{i2(p-n)x} J_0(k\sin x) \\ &= \int_0^\infty dk\, e^{-\mu_s k} \int_{\theta/2-\pi}^{\theta/2} dx\, \big[\cos(2[p-n]x) + i\sin(2[p-n]x)\big] J_0(k\sin x). \end{aligned} \tag{A.5}$$

To find the inner integral we use results from Gradshteyn and Ryzhik [92]

$$\begin{aligned} &\text{(6.681 6. p. 756)} \\ &\int_0^\pi dx\, J_0(2z\sin x)\cos 2nx = \pi J_n^2(z) \\ &\text{(6.681 8. p. 756)} \\ &\int_0^\pi dx\, \sin(2\mu x) J_{2\nu}(2a\sin x) = \pi\sin(\mu\pi) J_{\nu-\mu}(a) J_{\nu+\mu}(a), \\ &\qquad\qquad \operatorname{Re}\nu > -1. \end{aligned} \tag{A.6}$$

Although the integration limits are fixed to 0 and π (A.6) is still valid for calculating the inner integral of (A.5) since the integrand has a period of π and the length of the integration interval one period, therefore

$$\begin{aligned} &\int_{\theta/2-\pi}^{\theta/2} dx\, \cos(2[p-n]x) J_0(k\sin x) = \pi J_{p-n}^2(k/2) \\ &\int_{\theta/2-\pi}^{\theta/2} dx\, \sin(2[p-n]x) J_0(k\sin x) = \pi\sin([p-n]\pi) J_{n-p}(k/2) J_{p-n}(k/2) = 0. \end{aligned} \tag{A.7}$$

Inserting this into (A.5) we get

$$\begin{aligned} K_{pn}(\theta) &= \pi \int_0^\infty dk\, e^{-\mu_s k} J_{p-n}^2(k/2) \\ &= 2\pi \int_0^\infty dk'\, e^{-2\mu_s k'} J_{p-n}^2(k'), \end{aligned} \tag{A.8}$$

where we have performed the variable exchange $k/2 \to k'$. To evaluate this integral we turn to Gradshteyn and Ryzhik

$$\begin{aligned} &\text{(6.612 3. p. 730)} \\ &\int_0^\infty dx\, e^{-\alpha x} J_\nu(\beta x) J_\nu(\gamma x) = \frac{1}{\pi\sqrt{\gamma\beta}}\, Q_{\nu-\frac{1}{2}}\left(\frac{\alpha^2+\beta^2+\gamma^2}{2\beta\gamma}\right) \\ &\qquad\qquad \operatorname{Re}(\alpha \pm i\beta \pm i\gamma) > 0, \quad \gamma > 0, \quad \operatorname{Re}\nu > -\tfrac{1}{2}, \end{aligned} \tag{A.9}$$

where $Q(z)$ is the Lagrange function of the second kind [88]. The last condition only applies for $p-n>0$, however, from (A.5) we see that the integral K_{pn} only depends on the difference $p-n$ and furthermore that it is Hermitian $K^*_{pn}=K_{np}$. Therefore, it is sufficient to calculate the integral for $p-n>0$ and using the Hermiticity to obtain the results for the remaining combinations of p and n (for which $p-n<0$). The integral becomes

$$K_{pn}(\theta)=2\pi\int_0^\infty dk'\,e^{-2\mu_s k'}J^2_{p-n}(k')=2\,Q_{p-n-\frac{1}{2}}(2\mu_s^2+1)\qquad(p-n>0). \tag{A.10}$$

The argument for the Lagrange function is very close to unity when μ_s is small. The asymptotic form of $Q(x)$ in the vicinity of $x=1^+$ is given by [88]

$$Q_\nu(x)=-\gamma-\psi(\nu+1)-\tfrac{1}{2}\ln\left(\tfrac{x}{2}-\tfrac{1}{2}\right), \tag{A.11}$$

where γ is the Euler constant and $\psi(x)$ is the Euler psi function which obeys

$$\begin{aligned}\psi(x+1)&=\psi(x)+\frac{1}{x}\\ \psi\left(\tfrac{1}{2}\right)&=-\gamma-2\ln 2+2\end{aligned} \tag{A.12}$$

and can therefore be calculated recursively. Using (A.10) the two-electron integral can be written

$$\begin{aligned}\langle\phi_l\phi_n|\phi_m\phi_p\rangle&=\frac{1}{\pi^2 r_0}\int d\theta\,e^{i(l-m+n-p)\theta}\,Q_{p-n-\frac{1}{2}}(2\mu_s^2+1)\\ &=\frac{2}{\pi r_0}\,Q_{p-n-\frac{1}{2}}(2\mu_s^2+1)\,\delta_{l-m+n-p,0}\end{aligned} \tag{A.13}$$

leading to an analytic expression for the matrix elements of the Fock operator

$$\begin{aligned}F^\alpha_{lm}&=h_{lm}+\frac{e^2}{4\pi\epsilon_0\epsilon_r}\sum_{n,p}\rho^T_{pn}\,\langle\phi_l\phi_n|\phi_m\phi_p\rangle-\rho^\alpha_{pn}\,\langle\phi_l\phi_n|\phi_p\phi_m\rangle\\ &=h_{lm}+\frac{4E_0}{\pi}\frac{r_0}{a_0^*}\sum_{n,p}\delta_{l-m,p-n}\left[\rho^T_{pn}\,Q_{p-n-\frac{1}{2}}(2\mu_s^2+1)-\rho^\alpha_{pn}Q_{m-n-\frac{1}{2}}(2\mu_s^2+1)\right]\end{aligned} \tag{A.14}$$

Appendix B

Interaction Energy

The expression for the interaction part of the Fock matrix elements (A.14) can be worked further to yield a simple expression that casts light on the role of the screening constant μ_s. Inserting for the Lagrange function and simplifying the interaction matrix elements for spin α become (neglecting constants)

$$\langle\, l \,|\, \hat{V}^{\alpha}_{\rm int} \,|m\rangle = \sum_{n,p} \delta_{l-m,p-n}\Big[-\rho^{\beta}_{pn}(\gamma+\ln\mu_s)-\rho^{T}_{pn}\psi(p-n+\tfrac{1}{2})+\rho^{\alpha}_{pn}\psi(m-n+\tfrac{1}{2})\Big] \quad \text{(B.1)}$$

(interchange α and β for spin β). The Coulomb interaction

$$\frac{1}{2}\sum_{i\neq j}\frac{1}{r_0\sqrt{\sin^2([\theta_i-\theta_j]/2)+\mu_s^2}} \quad \text{(B.2)}$$

is rotationally invariant

$$\sin^2\left(\frac{\theta_i-\theta_j}{2}\right) = \sin^2\left(\frac{(\theta_i+\theta_0)-(\theta_j+\theta_0)}{2}\right) \quad \text{(B.3)}$$

and can therefore not couple states of different angular momentum. The Coulomb matrix is thus diagonal with elements

$$\begin{aligned}
\langle m|\, \hat{V}^{\alpha}_{\rm int} \,|m\rangle &= \sum_{n,p}\delta_{0,p-n}\Big[-\rho^{\beta}_{pn}(\gamma+\ln\mu_s)-\rho^{T}_{pn}\psi(p-n+\tfrac{1}{2})+\rho^{\alpha}_{pn}\psi(m-n+\tfrac{1}{2})\Big] \\
&= \sum_{n}\left[-\rho^{\beta}_{nn}(\gamma+\ln\mu_s)-\rho^{T}_{nn}\psi(\tfrac{1}{2})+\rho^{\alpha}_{nn}\psi(m-n+\tfrac{1}{2})\right] \\
&= -N^{\beta}_{e}(\gamma+\ln\mu_s)-N_e\psi(\tfrac{1}{2})+\sum_{n}\rho^{\alpha}_{nn}\psi(m-n+\tfrac{1}{2}) \\
&= -N^{\beta}_{e}(\gamma+\ln\mu_s+\psi(\tfrac{1}{2}))-N^{\alpha}_{e}\psi(\tfrac{1}{2})+\sum_{n}\rho^{\alpha}_{nn}\psi(m-n+\tfrac{1}{2})
\end{aligned} \quad \text{(B.4)}$$

The total interaction energy becomes

$$\begin{aligned} E_{\text{int}} &= E_{\text{int}}^{\alpha} + E_{\text{int}}^{\beta} = \sum_m \rho_{mm}^{\alpha} \langle m| \hat{V}_{\text{int}}^{\alpha} |m\rangle + \sum_m \rho_{mm}^{\beta} \langle m| \hat{V}_{\text{int}}^{\beta} |m\rangle \\ &= -2N_e^{\alpha} N_e^{\beta} (\gamma + \ln \mu_s + \psi(\tfrac{1}{2})) - \psi(\tfrac{1}{2}) \left[(N_e^{\alpha})^2 + (N_e^{\beta})^2 \right] \\ &\quad + \sum_m \rho_{mm}^{\alpha} \sum_n \rho_{nn}^{\alpha} \psi(m - n + \tfrac{1}{2}) + \sum_m \rho_{mm}^{\beta} \sum_n \rho_{nn}^{\beta} \psi(m - n + \tfrac{1}{2}) \end{aligned} \tag{B.5}$$

Appendix C

Orbital Magnetic Moment

The orbital magnetic moment of a system of electrons on a ring can be calculated exactly when the Coulomb interaction is neglected. The orbital magnetic moment of a system is defined as

$$M_o = \frac{1}{2}\int d\mathbf{r}\big[\mathbf{r}\times\big\langle\mathbf{J}(\mathbf{r})\big\rangle\big]\cdot\hat{\mathbf{n}} \tag{C.1}$$

where $\hat{\mathbf{n}}$ is a unit vector perpendicular to the plane of the system and $\big\langle\mathbf{J}(\mathbf{r})\big\rangle$ is the current density averaged over the Fermi distribution. The current density can be derived from the continuity relation by assuming a Hamiltonian of the form

$$H = \frac{\mathbf{p}^2}{2m} + V(\mathbf{r}) \tag{C.2}$$

and is given by

$$\mathbf{J}(\mathbf{r}) = -\frac{e}{2}\big[\mathbf{v}\,|\mathbf{r}\rangle\,\langle\mathbf{r}| + |\mathbf{r}\rangle\,\langle\mathbf{r}|\,\mathbf{v}\big], \tag{C.3}$$

where $\mathbf{v}$ is the effective velocity

$$\mathbf{v} = \frac{1}{m^*}\left(\mathbf{p} + e\mathbf{A}\right) = \frac{\hbar}{m^*}\left(-i\nabla + \frac{e}{\hbar}\mathbf{A}\right). \tag{C.4}$$

Using this definition the current of a state $|\psi_i\rangle$ is given by

$$\begin{aligned}
\mathbf{j}_i(\mathbf{r}) = \langle\psi_i|\,\mathbf{J}(\mathbf{r})\,|\psi_i\rangle &= -\frac{e}{2}\big[\langle\psi_i|\,\mathbf{v}\,|\mathbf{r}\rangle\,\langle\mathbf{r}|\psi_i\rangle + \langle\psi_i|\mathbf{r}\rangle\,\langle\mathbf{r}|\,\mathbf{v}\,|\psi_i\rangle\big] \\
&= -\frac{e}{2}\big[\mathbf{v}(\mathbf{r})\psi_i^*(\mathbf{r})\psi_i(\mathbf{r}) + \psi_i^*(\mathbf{r})\mathbf{v}(\mathbf{r})\psi_i(\mathbf{r})\big] \\
&= -e\,\mathrm{Re}\left\{\psi_i^*(\mathbf{r})\mathbf{v}(\mathbf{r})\psi_i(\mathbf{r})\right\} \\
&= -\frac{e\hbar}{m^*}\mathrm{Re}\left\{\psi_i^*(\mathbf{r})\left(-i\nabla + \frac{e}{\hbar}\mathbf{A}\right)\psi_i(\mathbf{r})\right\}.
\end{aligned} \tag{C.5}$$

The total current density is the sum of the currents of each state weighted by the occupation number

$$\big\langle\mathbf{J}(\mathbf{r})\big\rangle = \sum_i f(\varepsilon_i - \mu)\,\mathbf{j}_i(\mathbf{r}). \tag{C.6}$$

The magnetic moment is therefore

$$\begin{aligned} M_o &= \frac{1}{2}\int d\mathbf{r}\big[\mathbf{r}\times\big\langle\mathbf{J}(\mathbf{r})\big\rangle\big]\cdot\hat{\mathbf{n}} \\ &= -\frac{e\hbar}{2m^*}\sum_i f(\varepsilon_i-\mu)\int_0^{2\pi} r_0\,d\theta\,\hat{e}_z\cdot\left[\mathbf{r}\times\mathrm{Re}\left\{\psi_i^*(\mathbf{r})\left(-i\nabla+\frac{e}{\hbar}\mathbf{A}\right)\psi_i(\mathbf{r})\right\}\right] \\ &= -\frac{e\hbar r_0}{2m^*}\sum_i f(\varepsilon_i-\mu)\int_0^{2\pi} d\theta\,\hat{e}_z\cdot\left[\mathbf{r}\times\mathrm{Re}\left\{-i\psi_i^*(\mathbf{r})\nabla\psi_i(\mathbf{r})+\frac{e}{\hbar}\mathbf{A}\psi_i^*(\mathbf{r})\psi_i(\mathbf{r})\right\}\right]. \end{aligned} \tag{C.7}$$

The cross product can be done before taking the real part, and since

$$\begin{aligned} \mathbf{r}\times\nabla &= r_0\hat{e}_r\times\frac{1}{r_0}\frac{\partial}{\partial\theta}\,\hat{e}_\theta=\frac{\partial}{\partial\theta}\,\hat{e}_z \\ \mathbf{r}\times\mathbf{A} &= \mathbf{r}\times\left(-\frac{1}{2}\mathbf{r}\times\mathbf{B}\right)=\mathbf{r}\times\left(\frac{r_0B}{2}\,\hat{e}_\theta\right)=\frac{r_0^2B}{2}\,\hat{e}_z \end{aligned} \tag{C.8}$$

we therefore get (with $\hat{e}_z\cdot\hat{e}_z=1$)

$$M_o=-\frac{e\hbar r_0}{2m^*}\sum_i f(\varepsilon_i-\mu)\int_0^{2\pi}d\theta\,\mathrm{Re}\left\{-i\psi_i^*(\theta)\frac{\partial\psi_i}{\partial\theta}+\frac{er_0^2B}{2\hbar}\psi_i^*(\theta)\psi_i(\theta)\right\}. \tag{C.9}$$

Expanding $|\psi_i\rangle$ in the basis of $\hat{h}_0$ (2.10) as well as using

$$\mu_B^*=\frac{e\hbar}{2m^*}\,,\qquad m_\Phi=\frac{\Phi}{\Phi_0}=\frac{er_0^2B}{2\hbar} \tag{C.10}$$

the magnetic moment becomes

$$\begin{aligned} M_o = -\frac{\mu_B^*}{2\pi}\sum_i f(\varepsilon_i-\mu)\int_0^{2\pi}d\theta \\ \mathrm{Re}\left\{-i\sum_{l,m}c_{il}^*e^{il\theta}c_{im}\frac{\partial e^{-im\theta}}{\partial\theta}+m_\Phi\sum_{l,m}c_{il}^*c_{im}e^{i(l-m)\theta}\right\} \\ = \frac{\mu_B^*}{2\pi}\sum_i f(\varepsilon_i-\mu)\int_0^{2\pi}d\theta\,\mathrm{Re}\left\{\sum_{l,m}(m-m_\Phi)\,c_{il}^*c_{im}e^{i(l-m)\theta}\right\}. \end{aligned} \tag{C.11}$$

By interchanging the integration and summation and using

$$\int_0^{2\pi}d\theta\,e^{i(l-m)\theta}=2\pi\delta_{lm} \tag{C.12}$$

we get

$$\begin{aligned} M_o &= \mu_B^* \sum_i f(\varepsilon_i - \mu) \mathrm{Re} \left\{ \sum_{l,m} (m - m_\Phi)\, c_{il}^* c_{im}\, \delta_{lm} \right\} \\ &= \mu_B^* \sum_i f(\varepsilon_i - \mu) \mathrm{Re} \left\{ \sum_{m} (m - m_\Phi)\, c_{im}^* c_{im} \right\} \\ &= \mu_B^* \sum_m \sum_i f(\varepsilon_i - \mu) c_{im}^* c_{im}\, (m - m_\Phi) \\ &= \mu_B^* \sum_m \rho_{mm}\, (m - m_\Phi)\,. \end{aligned} \tag{C.13}$$

BIBLIOGRAPHY

[1] J. H. DAVIES, *The Physics of Low-Dimensional Semiconductors* (Cambridge University Press, Cambridge, 1998).

[2] F. BLOCH, *Off-Diagonal Long-Range Order and Persistent Currents in a Hollow Cylinder*, Phys. Rev. **137**, A787 (1965).

[3] M. SCHICK, *Flux Quantization in a One-Dimensional Model*, Phys. Rev. **166**, 404 (1968).

[4] F. BLOCH, *Flux Quantization and Dimensionality*, Phys. Rev. **166**, 415 (1968).

[5] L. GUNTHER AND Y. IMRY, *Flux quantization without off-diagonal long-range orger in a thin hollow cylinder*, Solid State Commun. **7**, 1391 (1969).

[6] M. BÜTTIKER, Y. IMRY, AND R. LANDAUER, *Josephson behaviour in small normal one-dimensional rings*, Phys. Lett. A **96**, 365 (1983).

[7] R. LANDAUER AND M. BÜTTIKER, *Resistance of Small Metallic Loops*, Phys. Rev. Lett. **54**, 2049 (1985).

[8] M. BÜTTIKER, *Small normal-metal loop coupled to an electron reservoir*, Phys. Rev. B **32**, 1846(R) (1985).

[9] Y. GEFEN, Y. IMRY, AND M. Y. AZBEL, *Quantum Oscillations and the Aharonov-Bohm Effect for Parallel Resistors*, Phys. Rev. Lett. **52**, 129 (1984).

[10] Y. AHARONOV AND D. BOHM, *Significance of Electromagnetic Potentials in the Quantum Theory*, Phys. Rev. **115**, 485 (1959).

[11] B. L. AL'TSHULER, A. G. ARONOV, AND B. Z. SPIVAK, Pis'ma Zh. Eksp. Teor. Fiz. **33**, 101 (1981), [JETP Lett. **34**, 94 (1981)].

[12] D. Y. SHARVIN AND Y. V. SHARVIN, Pis'ma Zh. Eksp. Teor. Fiz. **34**, 285 (1981), [JETP Lett. **34**, 272 (1981)].

[13] B. L. AL'TSHULER, A. G. ARONOV, B. Z. SPIVAK, D. Y. SHARVIN, AND Y. V. SHARVIN, Pis'ma Zh. Eksp. Teor. Fiz. **35**, 476 (1982), [JETP Lett. **35**, 588 (1982)].

[14] F. LADAN AND J. MAURER, C. R. Acad. Sci., Ser. II **296**, 1752 (1983).

[15] R. A. WEBB, S. WASHBURN, C. P. UMBACH, AND R. B. LAIBOWITZ, *Observation of h/e Aharonov-Bohm Oscillations in Normal-Metal Rings*, Phys. Rev. Lett. **54**, 2696 (1985).

[16] S. WASHBURN, C. P. UMBACH, R. B. LAIBOWITZ, AND R. A. WEBB, *Temperature dependence of the normal-metal Aharonov-Bohm effect*, Phys. Rev. B **32**, 4789 (1985).

[17] V. CHANDRASEKHAR, M. J. ROOKS, S. WIND, AND D. E. PROBER, *Observation of Aharonov-Bohm Electron Interference Effects with Periods h/e and h/2e in Individual Micron-Size, Normal-Metal Rings*, Phys. Rev. Lett. **55**, 1610 (1985).

[18] C. P. UMBACH, C. V. HAESENDONCK, R. B. LAIBOWITZ, S. WASHBURN, AND R. A. WEBB, *Direct Observation of Ensemble Averaging of the Aharonov-Bohm Effect in Normal Metal Loops*, Phys. Rev. Lett. **56**, 386 (1986).

[19] J. P. CARINI, K. A. MUTTALIB, AND S. R. NAGEL, *Origin of the Bohm-Aharonov Effect with Half Flux Quanta*, Phys. Rev. Lett. **53**, 102 (1984).

[20] D. A. BROWNE, J. P. CARINI, K. A. MUTTALIB, AND S. R. NAGEL, *Periodicity of transport coefficients with half flux quanta in the Aharonov-Bohm effect*, Phys. Rev. B **30**, 6798 (1984).

[21] M. GIJS, C. VAN HAESENDONCK, AND Y. BRUYNSRAEDE, Phys. Rev. Lett. **52**, 2069 (1984).

[22] M. GIJS, C. VAN HAESENDONCK, AND Y. BRUYNSRAEDE, Phys. Rev. B. **30**, 2964 (1984).

[23] B. Pannetier, J. Chaussy, R. Rammal, and P. Gandik, Phys. Rev. Lett. **53**, 718 (1984).

[24] B. Pannetier, J. Chaussy, R. Rammal, and P. Gandik, Phys. Rev. B **31**, 3209 (1985).

[25] A. D. Stone and Y. Imry, *Periodicity of the Aharonov-Bohm Effect in Normal Metal Rings*, Phys. Rev. Lett. **56**, 189 (1986).

[26] H.-F. Cheung, Y. Gefen, E. K. Riedel, and W.-H. Shih, *Persistent currents in small one-dimensional metal rings*, Phys. Rev. B **37**, 6050 (1988).

[27] G. Montambaux, H. Bouchiat, D. Sigeti, and R. Friesner, *Persistent currents in mesoscopic metallic rings: Ensemble average*, Phys. Rev. B **42**, 7647 (1990).

[28] L. P. Lévy, G. Dolan, J. Dunsmuir, and H. Bouchiat, *Magnetization of Mesoscopic Copper Rings: Evidence for Persistent Currents*, Phys. Rev. Lett. **64**, 2074 (1990).

[29] V. Chandrasekhar, R. A. Webb, M. J. Brady, M. B. Ketchen, W. J. Gallagher, and A. Kleinsasser, *Magnetic Response of a Single, Isolated Gold Loop*, Phys. Rev. Lett. **67**, 3578 (1991).

[30] D. Loss and P. Goldbart, *Period and amplitude halving in mesoscopic rings with spin*, Phys. Rev. B **43**, 13762 (1991).

[31] G. Timp, A. M. Chang, J. E. Cunningham, T. Y. Chang, P. Mankiewich, R. Behringer, and R. E. Howard, *Observation of the Aharonov-Bohm Effect for* $\omega_c\tau > 1$, Phys. Rev. Lett. **58**, 2814 (1987).

[32] D. Mailly, C. Chapelier, and A. Benoit, *Experimental Observation of Persistent Currents in a GaAs-AlGaAs Single Loop*, Phys. Rev. Lett. **70**, 2020 (1993).

[33] C. J. B. Ford, T. J. Thornton, R. Newbury, M. Pepper, H. Ahmed, C. T. Foxon, J. J. Harris, and C. Roberts, *The Aharonov-Bohm effect in electrostatically defined heterojunction rings*, J. Phys. C **21**, L325 (1988).

[34] C. J. B. FORD, T. J. THORNTON, R. NEWBURY, M. PEPPER, H. AHMED, D. C. PEACOCK, D. A. RITCHIE, J. E. F. FROST, AND G. A. C. JONES, *Electrostatically defined heterojunction rings and the Aharonov-Bohm effect*, Appl. Phys. Lett. **54**, 21 (1989).

[35] G. TIMP, P. M. MANKIEWICH, P. DEVEGVAR, R. BEHRINGER, J. E. CUNNINGHAM, R. E. HOWARD, H. U. BARANGER, AND J. K. JAIN, *Suppression of the Aharonov-Bohm effect in the quantized Hall regime*, Phys. Rev. B **39**, 6227 (1989).

[36] K. ISMAIL, S. WASHBURN, AND K. Y. LEE, *Conductance in very clean quantum wires and rings*, Appl. Phys. Lett. **59**, 1998 (1991).

[37] J. LIU, K. ISMAIL, K. Y. LEE, J. M. HONG, AND S. WASHBURN, *Cyclotron trapping, mode spectroscopy, and mass enhancement in small $GaAs/Al_xGa_{1-x}As$ rings*, Phys. Rev. B **47**, 13039 (1993).

[38] J. LIU, K. ISMAIL, K. Y. LEE, J. M. HONG, AND S. WASHBURN, *Correlations between Aharonov-Bohm effects and one-dimensional subband populations in $GaAs/Al_xGa_{1-x}As$ rings*, Phys. Rev. B **47**, 13039 (1993).

[39] C. DAHL, J. P. KOTTHAUS, H. NICKEL, AND W. SCHLAPP, *Magnetoplasma resonances in two-dimensional electron rings*, Phys. Rev. B **48**, 15480(R) (1993).

[40] J. LIU, W. X. GAO, K. ISMAIL, K. Y. LEE, J. M. HONG, AND S. WASHBURN, *Tunneling between edge states in clean multiple $GaAs/Al_xGa_{1-x}As$ rings and increase of the phase coherence length with magnetic field*, Phys. Rev. B **50**, 17383 (1994).

[41] S. PEDERSEN, A. E. HANSEN, A. KRISTENSEN, C. B. SÖRENSEN, AND P. E. LINDELOF, *Observation of quantum asymmetry in an Aharonov-Bohm ring*, Phys. Rev. B **61**, 5457 (2000).

[42] R. J. WARBURTON, C. SCHÄFLEIN, D. HAFT, F. BICKEL, A. LORKE, K. KARRAL, J. M. GARCIA, W. SCHOENFELD, AND P. M. PETROFF, *Optical emission from a charge-tunable quantum ring*, Nature **405**, 926 (2000).

[43] M. CASSÉ, Z. D. KVON, G. M. GUSEV, E. B. OLSHANETSKII, L. V. LITVIN, A. V. PLOTNIKOV, D. K. MAUDE, AND J. C. PORTAL, *Temperature dependence*

of the Aharonov-Bohm oscillations and the energy spectrum in a single-mode ballistic ring, Phys. Rev. B **62**, 2624 (2000).

[44] A. Fuhrer, S. Lüscher, T. Ihn, T. Heinzel, K. Ensslin, W. Wegscheider, and M. Bichler, *Energy spectra of quantum rings*, Nature **413**, 822 (2001).

[45] A. Lorke, R. J. Luyken, A. O. Govorov, J. P. Kotthaus, J. M. Garcia, and P. M. Petroff, *Spectroscopy of Nanoscopic Semiconductor Rings*, Phys. Rev. Lett. **84**, 2223 (2000).

[46] L. Wendler, V. M. Fomin, A. V. Chaplik, and A. O. Govorov, *Optical absorption and inelastic light scattering*, Phys. Rev. B **54**, 4794 (1996).

[47] V. Halonen, P. Pietiläinen, and T. Chakraborty, *Optical-absorption spectra of quantum dots and rings with a repulsive scattering centre*, Europhys. Lett. **33**, 377 (1996).

[48] J. Aizpurua, P. Hanarp, D. S. Sutherland, M. Käll, G. W. Bryant, and F. J. G. de Abajo, *Optical Properties of Gold Nanorings*, Phys. Rev. Lett. **90**, 057401 (2003).

[49] S. Viefers, P. S. Deo, S. M. Reimann, M. Manninen, and M. Koskinen, *Current-spin-density-functional study of persistent currents in quantum rings*, cond-mat/0005078 (2000).

[50] P. Koskinen and M. Manninen, *Persistent Currents in Small, Imperfect Hubbard Rings*, cond-mat/0310055 (2003).

[51] A. Müller-Groeling and H. A. Weidenmüller, *Persistent currents in one and two-dimensional mesoscopic rings: Influence of the Coulomb interaction, impurity scattering, and periodic potential*, Phys. Rev. B **49**, 4752 (1994).

[52] T. Chakraborty and P. Pietiläinen, *Persistent currents in a quantum ring: Effects of impurities and interactions*, Phys. Rev. B **52**, 1932 (1995).

[53] P. Pietiläinen, V. Halonen, and T. Chakraborty, *Electron correlations in quantum ring and dot systems*, Physica B **212**, 256 (1995).

[54] A. M. Jayannavar, P. S. Deo, and T. P. Pareek, *Current magnification and circulating currents in mesoscopic rings*, Physica B **212**, 261 (1995).

[55] S. BANDOPADHYAY, P. S. DEO, AND A. M. JAYANNAVAR, *Quantum current magnification in a multi-channel mesoscopic ring*, cond-mat/0312324 (2003).

[56] J. DESBOIS, S. OUVRY, AND C. TEXIER, *Persistent currents and magnetization in two-dimensional magnetic quantum systems*, Nucl. Phys. B **528**, 727 (1998).

[57] W.-C. TAN AND J. C. INKSON, *Magnetization, persistent currents, and their relation in quantum rings and dots*, Phys. Rev. B **60**, 5626 (1999).

[58] T. CHAKRABORTY AND P. PIETILÄINEN, *Electron-electron interaction and the persistent current in a quantum ring*, Phys. Rev. B **50**, 8460 (1994).

[59] H. KATO AND D. YOSHIOKA, *Suppression of persistent currents in one-dimensional disordered rings by the Coulomb interaction*, Phys. Rev. B **50**, 4943 (1994).

[60] D. YOSHIOKA AND H. KATO, *The effect of the Coulomb interaction on the mesoscopic persistent current*, Physica B **212**, 251 (1995).

[61] R. BERKOVITS AND Y. AVISHAI, *Interacting Electrons in Disordered Potentials: Conductance versus Persistent Currents*, Phys. Rev. Lett. **76**, 291 (1996).

[62] A. COHEN, K. RICHTER, AND R. BERKOVITS, *Spin and interaction effects on charge distribution and currents in one-dimensional conductors and rings within the Hartree-Fock approximation*, Phys. Rev. B **57**, 6223 (1998).

[63] K. NIEMELÄ, P. PIETILÄINEN, P. HYVÖNEN, AND T. CHAKRABORTY, *Fractional Oscillations of electronic states in a quantum ring*, Europhys. Lett. **36**, 533 (1996).

[64] F. V. KUSMARTSEV, J. F. WEISZ, R. KISHORE, AND M. TAKAHASHI, *Strong correlations versus U-center pairing and fractional Aharonov-Bohm effect*, Phys. Rev. B **49**, 16234 (1994).

[65] M. MANNINEN, P. KOSKINEN, M. KOSKINEN, P. S. DEO, S. M. REIMANN, AND S. VIEFERS, *Energy spectrum, persistent current and electron localization in quantum rings*, cond-mat/0311095 (2003).

[66] E. A. JAGLA AND C. A. BALSEIRO, *Electron-Electron Correlations and the Aharonov-Bohm Effect in Mesoscopic Rings*, Phys. Rev. Lett. **70**, 639 (1993).

[67] V. Gudmundsson, C. S. Tang, and A. Manolescu, *Non-adiabatic current generation in a finite-width semiconductor ring*, Phys. Rev. B **67**, 161301(R) (2003).

[68] C. S. Tang and C. S. Chu, *Quantum transport in the presence of a finite-range time-modulated potential*, Phys. Rev. B **53**, 4838 (1996).

[69] C. S. Tang and C. S. Chu, *Coherent quantum transport in narrow constrictions in the presence of a finite-range longitudinally polarized time-dependent field*, Phys. Rev. B **60**, 1830 (1999).

[70] S. Komlyama, O. Astafiev, V. Antonov, T. Kutsuwa, and H. Hiral, *A single-photon detector in the far-infrared range*, Nature **403**, 405 (2000).

[71] M. V. Moskalets, *Universal AC response of a 1D Luttinger liquid ring*, Phys. E **8**, 349 (2000).

[72] M. Moskalets and M. Büttiker, *Floquet states and persistent currents transitions in a mesoscopic ring*, Phys. Rev. B **66**, 245321 (2002).

[73] R. G. Mani, J. H. Smet, K. von Klitzing, V. Narayanamurti, W. B. Johnson, and V. Umansky, *Zero-resistance states induced by electromagnetic-wave excitation in GaAs/AlGaAs heterostructures*, Nature **420**, 646 (2002).

[74] V. Gudmundsson, C. S. Tang, and A. Manolescu, *Impurity and spin effects on the magneto-spectroscopy of a THz-modulated nanostructure*, Phys. Rev. B **68**, 165343 (2003).

[75] P. H. Rivera and P. A. Schulz, *Radiation induced zero-resistance states: a dressed electronic structure effect*, cond-mat/0305019 (2003).

[76] M. Moskalets and M. Büttiker, *Quantum pumping: Coherent Rings versus Open Conductors*, Phys. Rev. B **68**, 161311 (2003).

[77] S. N. Shevchenko, Y. V. Pershin, and I. D. Vagner, *Magnetization of Nuclear-Spin-Polarization-Induced Quantum Ring*, cond-mat/0309390 (2003).

[78] S. S. Gylfadottir, V. Gudmundsson, C. S. Tang, and A. Manolescu, *Non-adiabatic Current Excitation Quantum Rings*, cond-mat/0309661 (2003).

[79] G. P. ZHANG, *Hartree-Fock Dynamical Electron-Correlation Effects in C_{60} after Laser Excitation*, Phys. Rev. Lett. **91**, 176801 (2003).

[80] C. LUO, K. REIMANN, M. WOERNER, AND T. ELSAESSER, *Nonlinear terahertz spectroscopy of semiconductor nanostructures*, Appl. Phys. A **78**, 435 (2004).

[81] S. S. GYLFADOTTIR, M. NITA, V. GUDMUNDSSON, AND A. MANOLESCU, *Net current generation in a 1D quantum ring at zero magnetic field*, cond-mat/0402582 (2004).

[82] J. A. NESTEROFF, Y. V. PERSHIN, AND V. PRIVMAN, *Dynamic Quantum Wire*, cond-mat/0403448 (2004).

[83] S. WASHBURN AND R. A. WEBB, *Aharonov-Bohm effect in normal metal. Quantum coherence and transport*, Adv. Phys. **35**, 375 (1986).

[84] J. M. LUTTINGER, *Fermi Surface and Some Simple Equilibrium Properties of a System of Interacting Fermions*, Phys. Rev. **119**, 1153 (1960).

[85] V. FOCK, *Näherungsmethoden zur Lösung des Quantenmechanischen Mehrkörperproblems*, Z. Phys. **61**, 126 (1930).

[86] A. SZABO AND N. S. OSTLUND, *Modern Quantum Chemistry* (Dover Publications, Inc., Mineola, New York, 1996).

[87] J. A. POPLE AND R. K. NESBET, *Self-consistent orbitals for radicals*, J. Chem. Phys. **22**, 571 (1954).

[88] W. MAGNUS, F. OBERHETTINGER, AND R. P. SONI, *Formulas and Theorems for the Special Functions of Mathematical Physics*, vol. 52 of *Die Grundlehren der Mathematischen Wissenschaften in Einzeldarstellungen* (Springer Verlag, New York, 1966), 3rd ed.

[89] J. D. JACKSON, *Classical Electrodynamics* (John Wiley & Sons, New York, 1999), 3rd ed.

[90] S. K. MAITI, J. CHOWDHURY, AND S. N. KARMAKAR, *Strange behaviour of persistent currents in mesoscopic Hubbard rings*, cond-mat/0310556 (2003).

[91] C. COHEN-TANNOUDJI, B. DIU, AND F. LALOË, *Quantum Mechanics*, vol. 1 and 2 (Hermann, Paris and John Wiley & Sons Inc., New York, 1977).

[92] I. S. GRADSHTEYN AND I. M. RYZHIK, *Table of integrals, series and products* (Academic Press, San Diego, 1994), 5th ed.